



**HAL**  
open science

# Epoxiconazole profoundly alters rat brain and properties of neural stem cells

Hiba Hamdi, Imen Graiet, Salwa Abid-Essefi, Joel Eyer

## ► To cite this version:

Hiba Hamdi, Imen Graiet, Salwa Abid-Essefi, Joel Eyer. Epoxiconazole profoundly alters rat brain and properties of neural stem cells. *Chemosphere*, 2022, 288, pp.132640. 10.1016/j.chemosphere.2021.132640 . hal-03548879

**HAL Id: hal-03548879**

**<https://univ-angers.hal.science/hal-03548879>**

Submitted on 8 Jan 2024

**HAL** is a multi-disciplinary open access archive for the deposit and dissemination of scientific research documents, whether they are published or not. The documents may come from teaching and research institutions in France or abroad, or from public or private research centers.

L'archive ouverte pluridisciplinaire **HAL**, est destinée au dépôt et à la diffusion de documents scientifiques de niveau recherche, publiés ou non, émanant des établissements d'enseignement et de recherche français ou étrangers, des laboratoires publics ou privés.



Distributed under a Creative Commons Attribution - NonCommercial 4.0 International License

1           **Epoxiconazole profoundly alters rat brain and properties of neural stem cells**

2

3

4   Hiba Hamdi<sup>a, b</sup>, Imen Graiet<sup>a</sup>, Salwa Abid-Essefi<sup>a</sup>, Joel Eyer<sup>c \*</sup>

5

6

7   <sup>a</sup>Laboratory for Research on Biologically Compatible Compounds, Faculty of Dental  
8   Medicine, University of Monastir, Avicenne Street, 5019 Monastir, Tunisia.

9

10   <sup>b</sup>Higher Institute of Biotechnology, University of Monastir, Tunisia.

11

12   <sup>c</sup>Laboratoire Micro et Nanomédecines Translationnelles (MINT), Inserm 1066, CNRS 6021,  
13   Institut de Biologie de la Santé, Centre Hospitalier Universitaire, 49033 Angers, France.

14

15

16   **\*Corresponding author: Joel Eyer**

17   E-mail: joel.eyer@univ-angers.fr

18   Tel: 33 (0)2.44.68.84.88

19   Fax: 33(0)2.44.68.84.89

20

21

22

23 **Abstract**

24 Epoxiconazole (EPX), a widely used fungicide for domestic, medical, and industrial  
25 applications, could cause neurodegenerative diseases. However, the underlying mechanism of  
26 neurotoxicity is not well understood. This study aimed to investigate the possible toxic  
27 outcomes of Epoxiconazole, a triazole fungicide, on the brain of adult rats *in vivo*, and *in vitro*  
28 on neural stem cells derived from the subventricular zone of newborn *Wistar* rats. Our results  
29 revealed that oral exposure to EPX at these concentrations (8, 24, 40, 56 mg/kg bw  
30 representing respectively NOEL (no observed effect level), NOEL × 3, NOEL × 5, and NOEL  
31 × 7) for 28 days caused a considerable generation of oxidative stress in adult rat brain tissue.  
32 Furthermore, a significant augmentation in lipid peroxidation and protein oxidation has been  
33 found. Moreover, it induced an elevation of DNA fragmentation as assessed by the Comet  
34 assay. Indeed, EPX administration impaired activities of antioxidant enzymes and inhibited  
35 AChE activity. Concomitantly, this pesticide produced histological alterations in the brain of  
36 adult rats. Regarding the embryonic neural stem cells, we demonstrated that the treatment by  
37 EPX reduced the viability of cells with an IC<sub>50</sub> of 10 μM. It also provoked the reduction of  
38 cell proliferation, and EPX triggered arrest in G1/S phase. The neurosphere formation and  
39 self-renewal capacity was reduced and associated with decreased differentiation. Moreover,  
40 EPX induced cytoskeleton disruption as evidenced by immunocytochemical analysis. Our  
41 findings also showed that EPX induced apoptosis as evidenced by a loss of mitochondrial  
42 transmembrane potential ( $\Delta\Psi_m$ ) and an activation of caspase-3. In addition, EPX promoted  
43 ROS production in neural stem cells. Interestingly, the pretreatment of neural stem cells with  
44 the N-acetylcysteine (ROS scavenger) attenuated EPX-induced cell death, disruption of neural  
45 stem cells properties, ROS generation and apoptosis. Thus, the use of this hazardous material  
46 should be restricted and carefully regulated.

47

48

49 **Keywords:** Pesticide; Neural stem cells; Oxidative stress; DNA damage; Mitochondria;  
50 Cytoskeleton.

51 **Abbreviations:** bw: body weight; CAT: Catalase; EPX: Epoxiconazole; GPx: Glutathion  
52 Peroxidase; GST: Glutathion S Transferase; SOD: Superoxide Dismutase; MDA:  
53 Malondialdehyde; MMP: Mitochondrial Membrane Potential; NOEL: No Observed Effect

54 Level; NSCs: Neural Stem Cells; PC: Protein carbonyls; ROS: Reactive Oxygen Species;  
55 SVZ: Sub-ventricular Zone; NAC: N-acetylcysteine; Rh-123: Rhodamine 123.

56

57

## 58 **1. Introduction**

59 Epoxiconazole (EPX) belongs to the family of triazole fungicides, and it is frequently used in  
60 diverse sectors and in large quantities all over the world. The repeated use of this fungicide to  
61 control fungal diseases on a wide range of crops can generate a lot of residues, which in turn  
62 can lead to environmental contamination (Bertelsen et al., 2001; Xin et al., 2010). EPX is a  
63 persistent pollutant with a soil half-life of 354 days and its residual soil concentrations are  
64 approximately 110–350 µg/kg seven days after spraying of this compound (Passeport et al.,  
65 2011). The exposure to this fungicide can be generated via the ingestion of contaminated food  
66 and water, and can accumulate in various organs including the brain. The principal antifungal  
67 mechanism of action of this pesticide is the arrest of CYP51 activity, an essential enzyme for  
68 sterol biosynthesis in fungi (Zarn et al., 2003). Furthermore, triazole fungicides including  
69 EPX can provoke various toxicological effects in mammals, such as perturbation of  
70 mammalian steroidogenesis, production of craniofacial abnormalities, and birth  
71 malformations (Crofton, 1996; Menegola et al., 2005; Giavini and Menegola, 2010).  
72 Moreover, accumulating evidences in animals and human beings have proved the capacity of  
73 triazole pesticides to induce endocrine deregulation (Taxvig et al., 2007; De castro and Maia,  
74 2012), neurophysiological perturbations (Pearson et al., 2016), and malformations (Aleck and  
75 Bartley, 1997). Increasing evidences suggests a close relationship between maternal exposure  
76 to EPX with genital diseases (De castro and Maia, 2012), increased delayed embryonic death  
77 (Taxvig et al., 2007; Taxvig et al., 2008), and placental atrophy (Moreno et al., 2013;  
78 Stinchcombe et al., 2013).

79 Brain damage is one of the main health problem associated with EPX toxicity. Divers reports  
80 published by EPA (2006) indicated that triazole fungicides provoke a variety of undesirable  
81 effects on mammals, especially on the nervous system, including neuropathological lesions  
82 and alter brain weight of rodents. One molecular underlying mechanism of triazole fungicides  
83 is the alteration of the cellular influx of Ca<sup>2+</sup>, which consequently affects the normal function  
84 of dopaminergic system (Heusinkveld et al., 2013; Grace, 2016; Volkow et al., 2017).

85 As previously demonstrated by Hamdi et al. (2019a), other cellular pathways are influenced  
86 by the treatment with EPX like cell proliferation, cytoskeleton organization, mitochondrial  
87 morphology and functions, as well as DNA replication and repair. To further evaluate the  
88 mechanisms of brain damage induced by EPX *in vivo*, we have poisoned rats with increasing  
89 doses of this pesticide, in order to better describe the possible alterations caused by this

90 product. We then focused our attention on neural stem cells (NSC), as this group of immature  
91 cells is crucial for the renewal and proliferation of neurons, astrocytes, and oligodendrocytes  
92 (Gage and Temple, 2013). They persist within the brain of developing and adult mammals  
93 including humans, rodents and primates (Altman, and Das, 1965; Eriksson et al., 1998;  
94 Kukekov et al., 1999; Pencea et al., 2001). Any perturbation of NSCs fundamental properties  
95 may conduct to disturbance of the function and the morphology of the nervous system, which  
96 can lead to long-term behavioral or cognitive disorders (Aimone et al., 2014). Here, we show  
97 that the increased exposure of NSCs to EPX dramatically affects their ability to form  
98 neurospheres and to proliferate. These profound perturbations are caused by multiple cellular  
99 alterations, including the cytoskeleton network and mitochondria.

100 As previously shown by Hamdi et al. (2019a), the exposure to EPX can cause the oxidative  
101 stress. In fact, the brain is constantly sensitive to the aggression of free radicals, because of its  
102 elevated rate of oxygen utilization, high content of polyunsaturated lipids and low levels of  
103 antioxidant enzymes. The excessive generation of ROS can cause a veritable harm to the  
104 biological molecules like proteins, lipids, DNA, and also the metabolism (Nieradko-Iwanicka  
105 and Borzecki, 2015). Several studies reported that ROS stimulation plays a primordial role in  
106 proliferation and fate determination of neural stem cells into neurons or oligodendrocytes (Le  
107 Belle et al., 2011; Perez Estrada et al., 2014). However, too much ROS generation could  
108 induce cellular failure, eventually resulting to neuronal death, which has been described to be  
109 a crucial cause of cell senescence during neurodegenerative diseases (Loh et al., 2006). Here,  
110 we show that the imbalance between ROS and antioxidants is an essential mechanism caused  
111 by excessive exposure to EPX, which affects rat brain structures and functions, and is  
112 particularly toxic on neural stem cells. To our knowledge, this is the first time that such  
113 devastating effects of EPX on rat brain tissue and neural stem cells are reported.

114

115

## 116 **2. Materials and methods**

### 117 **2.1. Chemicals and reagents**

118 Epoxiconazole ((1-[[3-(2-chloropenyl)-2-(4-fluorophenyl) oxiranyl] ethyl]-1H-1, 2, 4 triazole,  
119 EPX) (purity 99.3%) and NAC (N-acetylcysteine) were purchased from Sigma–Aldrich (St.  
120 Louis, .MO, USA). Minimal essential medium- $\alpha$  (Thermo Fisher Scientific Life Sciences,  
121 Waltham, MA), D-glucose (Sigma-Aldrich, St. Louis, MO), sodium pyruvate, HEPES,  
122 penicillin/ streptomycin, B27 (Thermo Fisher Scientific Life Sciences), epidermal growth  
123 factor (EGF; Promega, Madison, WI). 2, 7-Dichlorofluoresce diacetate (DCFH-DA) was  
124 supplied by Molecular Probes (Cergy Pontoise, France). Tris-HCl, Low melting point agarose  
125 (LMA) and normal melting point agarose (NMA), Bradford’s reagent, sodium dodecyl sulfate  
126 (SDS), hydrogen peroxide ( $H_2O_2$ ), ethidium bromide (BET), glacial acetic acid,  
127 trichloroacetic acid (TCA), thiobarbituric acid (TBA), pyrogallol, guanidine hydrochloride,  
128 5,5-dithiobis-2-nitrobenzoic (DTNB), 2,4-dinitrochlorobenzene (CDNB), 2,4-  
129 dinitrophenylhydrazine (DNPH), sodium hydrogen phosphate ( $Na_2HPO_4$ ), disodium  
130 ethylenediaminetetraacetate ( $Na_2EDTA$ ), and glutathione reduced (GSH) were from Sigma-  
131 Aldrich (St. Louis, .MO, USA). All other used chemicals were of analytical grade.

### 132 **2.2. Embryonic NSCs culture preparation**

133 We conducted part of our study on primary cultures of neural stem cells (NSCs) taken from  
134 the subventricular area of the brain of neonatal (1-5 day-old) *Wistar* rats. These newborn rats  
135 come from the animal facility of the Faculty of Medicine (University of Angers, France). The  
136 cells were incubated for 7 days. Floating neurospheres were formed from stem cells after 5-7  
137 days of culture.

### 138 **2.3. Animals experiments**

139 Thirty adult male *Wistar* rats ( $169 \pm 10$  g) were purchased from the Central Pharmacy of  
140 Tunisia. They were put in acclimatization conditions for two weeks before starting the  
141 experiments. The rats were lodged in appropriate cages at temperature ( $25-30^\circ C$ ), a humidity  
142 level (40-60 %) and a photoperiod of light/dark (12h/12h). The animals were provided ad  
143 libitum with a commercial standard pellet diet (SNA, Sfax, Tunisia, main ingredients: corn,  
144 luzern, soy and lime carbonate) and drinking water.

145

146 The doses of EPX were chosen according to the value of the No Observed Effect Level  
147 (NOEL) of EPX in *Wistar* male rats after the daily exposure to 8 mg/kg bw for 90 days.

148 According to the World Health Organization (WHO), the NOEL represents a dose that  
149 reflects the actual average daily exposure in humans without observed adverse effects. One  
150 reason for the application of four dose levels ranging from a typical maximum allowed human  
151 exposure level above the reference value to a clear effect level was that the potential  
152 occurrence of effects at low doses has been postulated for triazoles.

153 The NOEL of EPX was set based on increased clinical liver parameters, hepatocyte  
154 hypertrophy, and increased liver weight. Indeed, in rats, in a 28-day oral study, no NOEL was  
155 set since increased clinical parameters indicating liver damage were shown even at the lowest  
156 dose (EFSA 2008a).

157 The rats were classified randomly into five groups (n = 6/group). The control batch (I)  
158 received orally the vehicle (corn oil), and the four other batches (II, III, IV and V) received  
159 for 28 days and by oral route EPX at these concentrations NOEL (8 mg/kg bw), NOEL × 3  
160 (24 mg/kg bw), NOEL × 5 (40 mg/kg bw) and NOEL × 7 (56 mg/kg bw). During the period  
161 of treatment the animals were weighted weekly with permanent death check, and the doses of  
162 EPX were prepared daily. At the end of experiments the animals were sacrificed by  
163 decapitation and the blood was taken by cardiac puncture. Finally, the blood samples were  
164 centrifuged and the resulted plasma was then stocked at -20°C until analysis.

#### 165 **2.4. Tissue preparation**

166 All rats were weighed and sacrificed at the end of the experiment period. The brains were  
167 immediately taken, cleaned with cold PBS, and weighed. For histological analysis, the intact  
168 brain tissues were fixed in 30 % buffered-neutral formalin and embedded in paraffin. Some  
169 portions of brain tissue used for biochemical analyses were immediately frozen at -20 °C until  
170 further processing. Before the measurements of oxidative stress parameters, the brain samples  
171 were homogenized with a Potter (glass Teflon) in cold Tris-HCl (10 mM, pH 7.4), and  
172 centrifuged at 13000 rpm and 4°C for 30 min to obtain a supernatant. The Bradford's reagent  
173 was used to determine protein concentration in brain tissue at 595 nm (Bradford, 1976). Other  
174 brain tissue portions used in the alkaline comet assay were isolated, cleaned from the adhering  
175 matters, put in cold PBS, carefully minced with scissors and glass rod into fine pieces, and the  
176 obtained cellular suspension was immediately used for preparation of agarose microgels.

#### 177 **2.5. Evaluation of the redox status in brain tissue**

### 178 **2.5.1. Evaluation of lipid peroxidation**

179 Lipid peroxidation in the brain tissue was quantified by the measurement of Malondialdehyde  
180 (MDA) levels according to the method of Ohkawa et al. (1979). Briefly, 200 µl of brain  
181 extract were combined with 200 µl of 8.1% SDS, 1.5 ml of 20% acetic acid adjusted to pH 3.5  
182 and 1.5 ml of 0.8% thiobarbituric acid. The final volume of the mixture was brought to a  
183 volume of 4 ml with distilled water and incubated in boiling water (95 °C) for 120 min. After  
184 cooling to room temperature with tap water, 5 ml of a mixture of n-butanol and pyridine  
185 (15:1, v:v) was added to each sample and the solution was shaken vigorously. Subsequently,  
186 samples were centrifuged at 4000 rpm for 10 min. The absorbance of the isolated supernatant  
187 fraction was measured at 546 nm. MDA concentrations were calculated according to a  
188 standard curve.

### 189 **2.5.2. Evaluation of protein oxidation**

190 Protein carbonyl content was determined in brain tissue homogenates by measuring the  
191 reactivity of carbonyl groups with 2,4-DNPH as described previously by Mercier et al.  
192 (2004). 200 µl of supernatant of brain homogenates, placed in glass tubes, were reacted with  
193 800 µl of 10 mM 2,4-DNPH in 2.5 M HCl for 1 h at room temperature in the dark and  
194 vortexed every 15 min. Samples were precipitated with 1 ml of 20% TCA and then tubes were  
195 left on ice for 10 min and centrifuged for 5 min at 4000 rpm to collect the protein precipitates.  
196 Another wash was done with 1 ml of 10% TCA and protein pellets were broken mechanically  
197 with the aid of a glass rod. The free 2,4-DNPH was removed by washing the pellets with 1 ml  
198 of ethanol-ethyl acetate. The final precipitates were solubilized in 500 µl of 6 M guanidine  
199 hydrochloride and kept at 37 °C for 10 min with general vortex mixing, and then centrifuged  
200 to remove any insoluble materials. The carbonyl content was determined  
201 spectrophotometrically at 370 nm, applying the molar extinction coefficient of 22.0 mM<sup>-1</sup>  
202 cm<sup>-1</sup>. A range of nmoles of carbonyls per ml is usually obtained for most proteins and is  
203 related to the protein content in the pellets.

### 204 **2.5.3. DNA fragmentation analysis**

205 Single cell gel electrophoresis (SCGE) is a visual and sensitive technique for measuring DNA  
206 breakage in individual mammalian cells. Each piece of the brain was placed in 0.5 ml of cold  
207 phosphate buffered saline (PBS, 20 mM EDTA, and 10% DMSO) and minced to obtain a  
208 cellular suspension. Cerebral cell suspension was embedded in 60 µl of 1% low melting point  
209 agarose and spread on agarose-precoated microscope slides. After agarose solidification, cells

210 were treated with an alkaline lysis buffer (2.5 M NaCl, 0.1 M EDTA, 10 mM Tris, pH 10, 1%  
211 (v/v) Triton X-100 and 10% (v/v) DMSO) for 1 h at 4 °C, then the DNA was allowed to  
212 unwind for 40 min in the electrophoresis buffer (0.3 M NaOH, 1 mM EDTA, pH > 13). The  
213 slides were then subjected to electrophoresis in the same buffer for 30 min at 25 V and 300  
214 mA. Slides were then neutralized using a Tris buffer solution (0.4 M Tris, pH 7.5) for 15 min.  
215 After staining the slides with ethidium bromide (20 µg/ml), the comets were detected and  
216 scored using a fluorescence microscope. The experiment was carried out in triplicate. The  
217 damage is represented by an increase of DNA fragments that have migrated out of the cell  
218 nucleus during electrophoresis and formed an image of a “comet” tail. A total of 100 comets  
219 on each slide were visually scored according to the intensity of fluorescence in the tail and  
220 classified by one of five classes as described by (Collins et al., 1996). The total score was  
221 evaluated with the following equation: (% of cells in class 0 × 0) + (% of cells in class 1 × 1)  
222 + (% of cells in class 2 × 2) + (% of cells in class 3 × 3) + (% of cells in class 4 × 4).

#### 223 **2.5.4. Assessment of superoxide dismutase (SOD) activity**

224 The SOD activity test is established on the autodegradation of pyrogallol (Marklund and  
225 Marklund, 1974). The inhibition of 50 % of pyrogallol auto-oxidation is proportional to one  
226 unit of SOD.

#### 227 **2.5.5. Evaluation of catalase activity**

228 The Catalase activity assay (CAT) was performed according to a previously published  
229 protocol of Acuna et al. (2009). The hydrogen peroxide (H<sub>2</sub>O<sub>2</sub>) was used as substrate and the  
230 optical density was quantified at 240 nm.

#### 231 **2.5.6. Evaluation of glutathione peroxidase activity**

232 The glutathione peroxidase activity assay (GPx) was performed according to the original  
233 procedure of Flohe and Gunzler, (1984). The diminution of reduced GSH level compared to  
234 the white reaction is proportional to the GPx activity.

#### 235 **2.5.7. Evaluation of glutathione S-transferase activity**

236 The enzymatic activity of glutathione-S-transferase (GST) was performed according to the  
237 original procedure of Habig et al. (1974). The generation of the chromophore (1-glutathione-  
238 2, 4-dinitrobenzene) is proportional to the activity of GST.

#### 239 **2.6. Evaluation of acetylcholinesterase activity**

240 The acetylcholinesterase (AChE) activity was performed according to the original procedure  
241 of Ellman et al. (1961). Measurement of this activity was based on the degradation of  
242 acetylcholine iodide as a substrate of AChE. The results were expressed as  $\mu\text{mol}$   
243 acetylthiocholine hydrolyzed/min/mg protein.

## 244 **2.7. Histological investigation**

245 In order to evaluate the possible histopathological alterations in the brain after EPX exposure,  
246 this organ was fixed in 30 % buffered formalin, dehydrated in increasing concentrations of  
247 alcohol and then dipped in paraffin (56 to 57°C). After cutting with a microtome, three slides  
248 were prepared from each group and for each coloration with Hematoxylin-Eosin. Each  
249 cerebral cortex slide was examined and assigned for severity of changes using scores on a  
250 scale of none (-), moderate (++) , and severe (+++) damages.

## 251 **2.8. Evaluation of embryonic neural stem cell viability**

252 The trypan blue exclusion technique was utilized to determine the neural stem cells viability.  
253 After seeding and treatment of 200-300 neurospheres with different doses of EPX or with  
254 colchicine (1 mg/ml) for 24 hours, NSCs were collected and mechanically dissociated. At the  
255 end, a Zeiss microscope was used to count the number of viable cells in each sample. On the  
256 other hand, in order to test the antioxidant effects of N acetylcysteine (NAC) against EPX-  
257 provoked neural stem cells mortality, the cells were preincubated with ROS scavenger (NAC,  
258 1 mM) for 2 hours before exposure to EPX at 10  $\mu\text{M}$  for 24 hours.

## 259 **2.9. Neural stem cell properties**

### 260 **2.9.1. Quantification of primary and secondary neurospheres**

261 The global amount of primary and secondary neurospheres was quantified according to the  
262 original method of Nicoleau et al. (2009). After seeding of NSCs in 24-well plates in culture  
263 medium containing 20 ng/ml EGF and treatment with or without EPX and colchicine, light  
264 microscopy was used to count the global amount of primary neurospheres after 5-7 of  
265 incubation.

266 The self-renewal assay is based on the collection of the previously formed neurospheres in  
267 each well and their dissociation into single cells in a new medium. After 5 days of incubation  
268 and with microscopic analysis the total number of secondary neurospheres for each condition  
269 was determined. The inverted microscope was used to observe the morphology of primary  
270 neurospheres.

### 271 **2.9.2. Analysis of neural stem cell proliferation**

272 Flow cytometry was used to analyze the cell cycle after treatment of NSCs with EPX for 24  
273 hours. In short, the neurospheres were grown into 6-well plates and exposed to EPX for 24  
274 hours at 37°C. After collection, centrifugation, mechanical dissociation and permeabilization  
275 with PBS-Tween of neurospheres, Ethanol 70% and RNase (1mg/ml) were added to samples  
276 for 30 minutes at 37°C. At the end, 10 mg/ml PI was added to each condition and cell  
277 distribution in the G1, S, and G2/M phases was evaluated.

### 278 **2.9.3. Analysis of neural stem cells differentiation by qRT-PCR**

279 The reverse transcription-polymerase chain reaction (qRT-PCR) assay was used to quantify  
280 the relative expression level of lineage-specific genes (NESTIN, TUBB3, GFAPa, and CNP).  
281 After treatment of cells with or without EPX for 4 days at 37°C, the neural stem cells were  
282 scraped, washed with PBS, and cryopreserved. A tissue sample weighting around 30 mg was  
283 added to 600 µl RLT buffer containing 10 µl β-mercaptoethanol per 1 ml. For homogenization  
284 of samples, tubes were placed into the adaptor sets, which are fixed into the clamps of the  
285 Qiagen tissue Lyser. Disruption was performed in a 2-min high-speed (30 Hz) shaking step.  
286 RNA concentration and purity from each sample were estimated using a Nanodrop 1000. The  
287 total RNA was then used as a template for one-step PCR using a 2× QuantiTect SYBR Green  
288 PCR Master Mix. Optimization of the sequence of the primers and the experimental protocol  
289 of qRT-PCR were performed by Plateforme d'Analyses Cellulaire et Moléculaire (PACEM),  
290 University of Angers as previously described (Lépinoux-Chambaud et al. 2016). The 25 µl  
291 RT-PCR reaction mixtures contained 12.5 µl of the 2× QuantiTect SYBR Green PCR Master  
292 Mix, 0.25 µl of RevertAid Reverse Transcriptase (200 U/µl), 0.5 µl of each forward and  
293 reverse primer of 10 pmol concentration, 10.25 µl of water, and 1 µl of RNA template. The  
294 reaction was performed in a Stratagene MX3005P real-time PCR machine. The thermal  
295 cycling conditions consisted of reverse transcription at 50 °C for 30 min, initial denaturation  
296 at 95 °C for 15 min and amplification for 40 cycles of denaturing at 94 °C for 15 s, annealing  
297 at 60 °C for 30 s and elongation at 72 °C for 30 s. Each sample was measured in triplicate. A  
298 melting curve analysis was performed following PCR amplification. The amplification curves  
299 and CT values were determined by the Stratagene MX3005P software. All of the different  
300 RT-PCR processes and reporting comply with MIQE guidelines. The expression level of the  
301 target genes was normalized to that of -specific glyceraldehyde-3-phosphate dehydrogenase  
302 mRNA, and the relative fold changes in gene expression were calculated based on the  
303  $2^{-\Delta\Delta CT}$  comparative method.

## 304 **2.10. ROS production measurements**

305 Neural stem cells were grown in 96-well black plates at 37 °C, and exposed to increasing  
306 doses of EPX (2, 5 and 10 µM). After PBS wash, centrifugation to eliminate EPX, 20 µM  
307 2',7'- dichlorofluoresceindiacetate (DCFDA) was put in each well for 30 min. The  
308 fluorescence was quantified using a fluorimeter (Biotek FL800x) with an excitation  
309 wavelength of 485 nm and emission wavelength of 522 nm. The DCF fluorescence intensity  
310 is proportional to the intracellular ROS content.

## 311 **2.11. Immunofluorescence analysis**

312 In order to show the possible effect of EPX on the cytoskeleton organization, especially on  
313 the microtubule network of NSCs, 200 neurospheres were grown for 24 hours on coverslips in  
314 24-well plate. After treatment with EPX (2, 5, and 10 µM) or colchicine for 3 hours, PBS  
315 wash, fixation with paraformaldehyde and PBS re-wash, 0.5% Triton X-100 permeabilization  
316 solution was added to each condition for 30 minutes. Then, the neurospheres were washed in  
317 PBS and incubated in a blocking solution (1% bovine serum albumin in 0.1% Triton X-100)  
318 for 1 hour, and the mouse anti-alpha-tubulin antibody diluted 1/1,000 was incubated with the  
319 neurospheres overnight at 4°C. The revelation of tubulin was done by Alexa Fluor 568-labeled  
320 anti-mouse antibody at 1/200 dilution for 2 hours. After three times PBS wash, the 9,6-  
321 diamidino-2-phenylindole (DAPI) for 5 minutes was added to each well. At the end, the  
322 montage of the coverslips was done using a ProLong Gold anti-fade solution and the  
323 morphology of neurospheres was visualized using confocal microscopy (Leica TCS SP8).

## 324 **2.12. Mitochondrial morphology**

325 Mito-tracker Red CMXRos was utilized to stain mitochondria. In short, after removal of  
326 culture medium and PBS wash containing 100 nM MitoTracker Red CMXRos probe, the  
327 mitochondrial morphology in NSCs was investigated by confocal microscopy.

## 328 **2.13. Mitochondrial membrane potential (TMRE /Rhodamine 123 Staining)**

329 In order to measure the Mitochondrial membrane potential (MMP), neural stem cells were  
330 stained with TMRE (the cationic probe). Briefly, neural stem cells (10<sup>4</sup> cells/ml) were seeded  
331 onto Ibidi 4 well slides, treated with EPX at different concentrations (2, 5, and 10µM) for 3  
332 hours, and incubated with TMRE solution (100 nM) for 15 min at 37 °C according to the  
333 manufacturer's instructions and observed by confocal microscopy.

334 We have also evaluated the MMP by using the probe Rhodamine 123 (Rh-123). The neural  
335 stem cells were grown in 96-well culture plates. After that, they were exposed and incubated  
336 for 24 h to different concentrations of EPX. Then, the medium was eliminated and the NSCs  
337 were incubated with 5 mM of Rh-123, and then rinsed and re-incubated with PBS. The  
338 decrease in the intensity of the fluorescence reflects the decrease in the retention of Rh-123  
339 and thus the fall of the mitochondrial potential.

#### 340 **2.15. Flow cytometric exploration**

341 FITC Annexin V/PI dyes combination was utilized to detect cell death. In short, neural stem  
342 cells were grown in 6-well plates ( $10^6$  cells/ml), exposed to EPX at (2, 5 and 10  $\mu$ M),  
343 trypsinized, resuspended in binding buffer and centrifuged. Then, the cells were exposed to  
344 Annexin V-FITC. Finally, Propidium Iodide was put in each sample. The result was examined  
345 by flow cytometry.

#### 346 **2.16. Evaluation of Caspase 3 activity**

347 Caspase-3 (active) Kit was used to assess caspase-3 activity (ab65613). Briefly, neural stem  
348 cells ( $10^6$  cells/ml) were grown in 6-well plates and exposed to EPX (2, 5, and 10  $\mu$ M). After  
349 24 h, an aliquot of 300  $\mu$ l of each sample was put into Eppendorf tubes. 2  $\mu$ l of the FITC-  
350 DEVD-FMK reagent was added to each condition for 1 hour. Then, a centrifugation of NSCs  
351 at 3000 rpm for 5 minutes and a remove of supernatant were effectuated. At the end, the cells  
352 were re-suspended in 0.5 ml of Wash Buffer and centrifuged again. Caspase activation was  
353 determined using flow cytometry.

#### 354 **2.17. Statistical analysis**

355 Data were examined using the Statistical Package for Social Sciences (SPSS, version 21). The  
356 one-way analysis of variance (ANOVA) following by Dunnett's post hoc comparisons was  
357 used to determine the statistical significance. Each experiment was repeated 3 times under  
358 different treatment conditions and data are expressed as the mean  $\pm$  SD. Values are  
359 significantly different (\*P < 0.05); (\*\*P < 0.001); (\*\*\*)P < 0.0001) from control.

360

### 361 **3. Results**

362 We first explored the *in vivo* impacts of EPX on the brain of male rats and after described the  
363 *in vitro* impact of the EPX exposure on the potential properties of neural stem cells, the  
364 oxidative stress generation, and on programmed cell death induction.

#### 365 **3.1. Absolute, and relative brain weights**

366 No abnormal mortality was found in any group during the treatment period. Nonetheless,  
367 Epoxiconazole treatment induced behavioral changes in rats like hypoactivity and weakness,  
368 loss of equilibrium, abnormal breathing and head bobbing. We have previously shown in  
369 Hamdi et al. (2019b) that the body weight of rats was increased as compared to the controls.  
370 Indeed, the absolute and relative weights of the brain (brain weight per 100 g of body weight)  
371 were significantly increased after the treatment with EPX (Fig. 1A). The evaluation of the  
372 organ weight from animal experiments aims to assess the current weight of the organ  
373 (absolute weight), and the relative weight which is expressed as proportions of the body  
374 weight of the animals.

#### 375 **3.2. Oxidative stress biomarkers**

376 The morphological alterations provoked by Epoxiconazole in brain tissue of rats can be  
377 explained by a perturbation of the normal redox state of this organ. Indeed, it is well  
378 recognized that oxidative stress is the main mechanism of pesticides toxicity (Hattab et al.,  
379 2015; Narra et al., 2017).

##### 380 **3.2.1. Assessment of lipid peroxidation**

381 Lipids are the principal targets of free radicals attack. Our findings indicated that the exposure  
382 to EPX at these concentrations (NOEL (8mg/kg bw), NOEL × 3 (24 mg/kg bw), NOEL × 5  
383 (40 mg/kg bw) and NOEL × 7 (56 mg/kg bw) strongly enhanced the MDA rates in brain  
384 tissue (Fig. 1B).

##### 385 **3.2.2. Evaluation of protein oxidation**

386 We assessed the effect of EPX treatment on protein oxidation in the brain of male rats after 28  
387 days of EPX intoxication, and found that EPX treatment significantly increased the formation  
388 of carbonylated proteins (Fig. 1C). We have found an increase in the amount of carbonyl  
389 groups from  $60 \pm 0.51$  in the control group to  $120 \pm 0.4$  nmol of carbonyl group/mg of

390 proteins in the group treated with the highest concentration (56 mg/kg bw) of EPX ( $p < 0.05$   
391 or  $p < 0.000$ ).

### 392 **3.2.3. DNA damage**

393 Exposure to pesticides frequently provokes genotoxic effects resulting in mutations and DNA  
394 fragmentation (Bolognesi, 2003). The comet assay is used to quantify the DNA alterations in  
395 biological systems (Tsuda et al., 1998). The level of DNA fragmentation in the brains of rats  
396 after administration of increased concentrations of EPX was estimated, and showed that the  
397 rate of DNA damage reached approximately 7 folds the control value for the brain (Fig. 1D)  
398 ( $p < 0.000$ ).

### 399 **3.2.4. Measurement of the antioxidant enzymes activity**

400 The antioxidant defense system performs a primordial function in maintaining cell  
401 homeostasis. In fact, we tested the impact of EPX on the activities of antioxidant enzymes and  
402 our data demonstrated that the activities of SOD, CAT, GPx, and GST were strongly  
403 enhanced in a dose dependent manner in the brain of treated groups (Fig. 2A-D) in  
404 comparison with the control group. Moreover, a decrease of the activities of these enzymes  
405 was found with the strongest concentration of EPX (56 mg/kg bw) except for SOD activity  
406 (Fig. 2B).

### 407 **3.3. AChE activity**

408 AChE is a key enzyme of the cholinergic system (Silman and Sussman, 2005). Indeed, divers'  
409 reports have reported the implication of AChE in the degradation of lipid peroxides (Fuhrman  
410 et al., 2004), and the exhaustion of this enzyme can be considered as an indicator of increased  
411 ROS generation. We have demonstrated that EPX treatment induces a significant decrease of  
412 AChE activity in the brain tissue of adult rats (Fig. 3A).

### 413 **3.4. Histological examinations**

414 The cerebral cortex of control rats presented regular histological structures (Fig. 3B1-3).  
415 However, in the treated groups, the cerebral cortex showed severe histological alterations. In  
416 particular, after EPX exposure the cerebral cortex showed characteristic dilations of blood  
417 vessels following H&E staining (Fig. 3B4), as well as vacuolated neurons (Fig. 3B5-6). There  
418 were also multiple inflammation patterns and oedema (Fig. 3B7), neuronal degeneration (Fig.

419 3B8) and hemorrhage (Fig. 3B9). These histological perturbations were categorized and  
420 presented in Table 1.

### 421 **3.5. Epoxiconazole inhibits cell viability of embryonic neural stem cell**

422 Accumulating evidences indicated that neural stem cells (NSCs) mobilization can be  
423 considered as a potential therapy to increase the survival of existing neurons against  
424 neurodegenerative disorders (Tincer et al., 2016). The proprieties of NSCs such as  
425 proliferation, renewal, and differentiation can be affected by different factors (Gao and Gao,  
426 2007; Anthony et al., 2008). On this basis, we explored the possible effects of EPX on NSCs,  
427 as one of main useful research tool for screening environmental neurotoxicants. Firstly, we  
428 tested the possible impact of EPX on NSCs. In order to investigate the effect of EPX on cell  
429 viability, we exposed rat isolated NSCs to increasing concentrations of EPX for 24 hours and  
430 used the Trypan blue exclusion technique to evaluate the cells. As shown in Fig. 4A, EPX  
431 significantly inhibited the cell viability after 24 hours of treatment.

### 432 **3.6. Epoxiconazole affects neural stem cells properties**

433 To better characterize EPX-affected neural stem cells proprieties, we evaluated the effects of  
434 EPX exposure on the fundamental characters of neural stem cells. Our results showed that the  
435 treatment of NSCs for 7 days with EPX provokes a clear modification of the typical spherical  
436 shape of neurospheres and increased the number of dissociated cells (Fig. 4B). Indeed, the  
437 exposure of NSCs to different concentrations of EPX strongly inhibited the number of  
438 primary (Fig. 4C) and secondary (Fig. 4D) neurospheres in a dose-dependent manner.  
439 Colchicine (5 µg/ml) was used as a positive control and we have found that it blocks the  
440 formation of both primary and secondary neurospheres formation (Fig. 4C-D). In summary,  
441 our findings show that EPX presents a great impact on the formation of primary neurospheres  
442 and it affects their self-renewal. The reduction of the self-renewal of NSCs was accompanied  
443 by a serious perturbation of their proliferation after EPX treatment (Fig. 5A). We observed the  
444 arrest of cells in G0/G1 phase accompanied by the inhibition of DNA synthesis in S phase  
445 using flow cytometry.

446 Interestingly, qRT-PCR investigation showed that the incubation of NSCs with EPX for 4  
447 days affects significantly their differentiation. We have found a significant decrease of  
448 expression of the neural stem cell-lineage specific gene (Nestin), the neuronal lineage marker  
449 (TUBB3), the astrocytic-lineage marker (GFAPa) and the premature oligodendrocyte-lineage

450 marker (CNP) after treatment of NSCs with 2, 5 and 10  $\mu\text{M/L}$  of EPX. Together, our results  
451 show that EPX strongly induces the arrest of the different NSC differentiation pathways (Fig.  
452 5B).

### 453 **3.7. Exposure to epoxiconazole induces oxidative stress in NSCs**

454 Several studies showed that the EPX toxicity mechanisms are related to the oxidative stress  
455 (Schwarzbacherová et al., 2017; Hamdi et al., 2018; Hamdi et al., 2019a). In our study, the  
456 treatment of NSCs with low concentrations of EPX (2, 5, and 10  $\mu\text{M}$ ) produces the generation  
457 of ROS in a dose depend manner (Fig. 5C).

### 458 **3.8. Epoxiconazole induces profound alterations to the microtubule network of NSCs**

459 Excessive ROS generation can interact with organelles like the cytoskeleton, which in turn  
460 can cause cell shape alteration and cytoskeleton degradation. Microscopic examination  
461 demonstrated that EPX provokes profound alterations of the microtubule (MTs) organization  
462 of NSCs. In untreated cells, a clear and normal organization of MTs is observed, but after 3 h  
463 of treatment by EPX, a remarkable disorganization of MTs was observed at 2  $\mu\text{M}$ . At higher  
464 concentration (5  $\mu\text{M}$ ), most of the MTs are degraded with formation of aggregates of tubulin.  
465 Finally, the microtubule network completely disappeared when treated with 10  $\mu\text{M}$  (IC50) of  
466 EPX (Fig. 5D).

### 467 **3.9. Epoxiconazole induces mitochondrial failure**

468 Accumulating evidences have demonstrated the close relationship between the mitochondrial  
469 dynamics and the neural stem cell destiny, and any disturbance of mitochondrial dynamics  
470 can affect the homeostasis of stem cells and their self-renewal ability (Khacho et al., 2016;  
471 Wang et al., 2018). In view of the key role of mitochondria in the normal cell functions, we  
472 investigated the influence of EPX on mitochondrial morphology. The MitoTracker CMXRos  
473 was used to stain the mitochondria. The microscopic analysis demonstrated that EPX  
474 treatment induced mitochondrial fragmentation (Fig. 6A). As several studies have indicated  
475 the crucial connection between oxidative stress generation and mitochondrial forms and  
476 functions failure (Lin and Beal, 2006 and Murphy, 2013), we analyzed the mitochondrial  
477 membrane potential using TMRE and Rh-123 staining to determine whether EPX causes  
478 mitochondrial dysfunction. Our results showed that EPX induces significantly the collapse of  
479 mitochondrial membrane potential, which is considered to be a characteristic of the onset of

480 the intrinsic apoptotic pathway. These results indicate that EPX provokes major mitochondrial  
481 dysfunction in NSCs (Fig. 6B).

### 482 **3.10. Epoxiconazole induces neural stem cell death by apoptosis**

483 In order to confirm the onset of programmed cell death, we co-stained cells with Annexin V  
484 FITC and PI. Our results show that EPX increases the rate of early and late apoptosis. After  
485 24h of EPX intoxication with the strongest dose, the percentage of apoptotic cells reached  
486 about 13 folds compared to the control rate. Also, as presented in Fig. 6C, EPX produced  $10.8$   
487  $\pm 0.3$ ,  $28.1 \pm 0.9$  and  $42.0 \pm 0.8$  of total rate of apoptosis at doses of 2, 5 and 10  $\mu\text{M}$   
488 respectively, as compared to  $3.0 \pm 0.2$  in untreated cells. Moreover, we examined the caspase-  
489 3 activity to confirm the implication of caspases on EPX-induced apoptosis. Figure 6D  
490 showed that EPX induces the activation of caspase-3 in a dose-dependent manner. The rate of  
491 cleaved caspase-3 was  $1.4 \pm 0.4$  % in untreated NSCs, and was  $8.42 \pm 0.8$ ,  $15.03 \pm 0.4$  and  
492  $27.05 \pm 0.9$  % in NSCs treated with respectively 2, 5 and 10  $\mu\text{M}$  of EPX.

### 493 **3.11. N-acetylcysteine prevents neural stem cells from EPX-induced programmed cell** 494 **death**

495 In order to show the implication of ROS generation in EPX-induced neural stem cells  
496 properties disruption and apoptosis, the cells were pre-incubated with NAC (1 mM) 2 hours  
497 before adding EPX (10  $\mu\text{M}$ ) for 24 hours, and the effect of the antioxidant (NAC) on EPX-  
498 induced cell viability inhibition was evaluated. The cell survival was increased from  $51.2 \pm$   
499  $0.05$  % in the group treated with EPX alone (10  $\mu\text{M}$ ), to  $88.1 \pm 0.08$  % in the group treated  
500 with EPX+ NAC (Fig. 7A). As compared to EPX alone, the pretreatment with NAC restored  
501 the amount of primary and secondary neurospheres (Fig. 7B-C). In addition, pretreatment  
502 with NAC reduced the loss of mitochondrial membrane potential (Fig. 6D), abolished the  
503 ROS generation (Fig. 7E) and strongly decreased the rate of apoptosis (Fig. 7F). Thus, ROS  
504 generation represents a major molecular mechanism involved in EPX-induced neural stem  
505 cell disruption and apoptotic cell death.

506

507

#### 508 **4. Discussion**

509 The widespread use of triazole fungicides in agriculture and for public health purposes has led  
510 to severe effects in many non-target species, including humans. Among triazole fungicides,  
511 Epoxiconazole can cross the blood-brain barrier, which can cause permanent harm to the  
512 brain tissue (Chambers et al., 2013). Nevertheless, the impact of Epoxiconazole on the  
513 nervous system and the possible underlying mechanisms are still unclear. Thus, our study was  
514 conducted to test the neurotoxic effects of EPX *in vivo* with a mechanistic focus on embryonic  
515 neural stem cell properties, oxidative injury, and apoptosis.

516 In toxicological studies, organ weight is an important criterion for the assessment of toxicity.  
517 The EPX administration induced significant increases in the absolute and the relative weights  
518 of the brain of adult rats, which could account for the edema and vacuolization shown in the  
519 histoarchitecture of rat cerebrum. This might be the result of an increased generation of free  
520 radicals, probably generated by EPX, and the subsequent installation of oxidative stress in the  
521 brain tissue of adult rats. Indeed, free radicals might attack polyunsaturated fatty acid (PUFA)  
522 of cell membranes causing destabilization, disintegration, fluidity alteration, and enhanced  
523 membrane permeability leading therefore to vacuolization, a primary response to cell injury  
524 (Robbins and Angel, 1976). The brain is more vulnerable to oxidative insults due to high rate  
525 of oxygen utilization and poor capacity to scavenge free radical species because of low  
526 concentration of antioxidants and related enzymes (Sayre et al., 2008). Thus, this weak organ  
527 is highly sensitive to free radicals aggression, which in turn can produce undesirable and  
528 irreversible damages to lipids, proteins, and DNA. In our study, we have evaluated the levels  
529 of lipid peroxidation and the oxidation of proteins in brain tissue, after exposure of adult rats  
530 to EPX, and our investigation showed that EPX provokes significant increases in the rate of  
531 malondialdehyde (MDA) and protein carbonyls (PCs) respectively. Our findings are in line  
532 with previous finding of Tabassum et al. (2016), which showed that the exposure to  
533 propiconazole, another triazole fungicide induces an augmentation of lipid peroxidation and  
534 protein oxidation level in the brain of freshwater fish *Channa punctata* Bloch. DNA is  
535 vulnerable to free radical's attack caused by the exposure to environmental pollutants, and the  
536 DNA fragmentation is an important marker of cell death caused by apoptosis. The current  
537 study showed that EPX induced DNA fragmentation in the brain of male rats. These results  
538 are in line with the previous finding of Elhady et al., (2019), which indicated that the exposure  
539 to Propiconazole for 2 months induces elevated rate of DNA damage in the brain of Sprague-  
540 Dawley rats. Moreover, to counteract the harm resulted by the excessive ROS production, the

541 cells will induce the activation of an endogenous defense system such as superoxide  
542 dismutase (SOD), glutathione peroxidase (GPx), catalase (CAT), and glutathione S  
543 transferase (GST). In this study, we found a considerable augmentation in CAT, SOD, GPx,  
544 and GSTs activities in the brain tissue of male rats following EPX intoxication. The  
545 augmentation of cerebral antioxidant system might be due to an important production of free  
546 radicals induced by EPX administration. Similarly, according to the study of Valadas et al.  
547 (2019), which indicated that exposure to Propiconazole at different concentrations increases  
548 the actions of antioxidant enzymes in zebrafish nervous system. On the other hand, the  
549 exposure of rats to the highest concentration of EPX (56 mg/kg bw), induced a decrease in the  
550 activities of CAT, GPx, and GST except for SOD activity. The considerable decline may be  
551 due to the maximum generation of ROS and the depletion of the antioxidant enzymes  
552 activities in the brain tissue of adult rats.

553 We focused our study on male adult rats to avoid possible effects due to the phase of the  
554 menstrual cycle including different plasma levels of sex hormones. However, to test  
555 Epoxiconazole in female animals could represent a new and very interesting investigation, not  
556 only to see if there is a difference between males and females, but also to see if this could  
557 affect their offspring.

558 The outcomes of EPX intoxication on nervous system function were also assessed by the  
559 evaluation of acetylcholinesterase (AChE) activity. AChE is mainly expressed in the nervous  
560 system and different isoforms of this enzyme are expressed in various tissues, including the  
561 liver and kidney. This enzyme is involved in the transmission of cholinergic synapses (Silman  
562 and Sussman 2005). It hydrolyzes the neurotransmitter acetylcholine (ACh) to choline and  
563 Acetyl-CoA. Reducing AChE activity improves cholinergic activity by increasing the level of  
564 ACh. Thus, ACh continually affects the receptor and causes cholinergic nervous excitability  
565 (Gu et al. 2015). Inhibition of AChE causes the accumulation of ACh which interferes with  
566 the function of the nervous system and eventually leads to respiratory failure and death  
567 (Worek et al.; 2002). In fact, it is well known that AChE activity is vital to normal behavior  
568 and muscular function. Furthermore, it has been demonstrated that AChE deficit leads to  
569 muscular alterations including the contractile properties and the lack of resistance to fatigue  
570 (Mouisel et al., 2006). Cholinergic neurotransmission in the brain also plays a central role in  
571 vigilance, learning, and memory. Our findings showed that treatment of rats with EPX  
572 impaired the cholinergic function of the brain as evidenced by a significant reduction of  
573 AChE activity. The inhibition of AChE activity in the brain of EPX-treated rats could

574 possibly explain the observed behavioral impairments like hypoactivity and weakness, loss of  
575 equilibrium and head bobbing. Similar results indicated that exposure to Penconazole during  
576 9 days affects the cholinergic function by decreasing the AChE activity in this organ of *Wistar*  
577 male rats (Chaâbane et al., 2016). The disruption of the cholinergic function in the brain of  
578 rats following EPX exposure appears to be the consequence of an important production of  
579 ROS. Brain histology is a major approach in evaluating the impact of EPX on brain failure.  
580 Our results showed that the exposure to this triazole fungicide caused marked perturbations in  
581 the global histo-architecture of the cerebral cortex as evidenced by haemorrhage, lipid  
582 vacuolation, oedema, inflammation, dilation of blood vessels, and neuronal degeneration. All  
583 these hazardous effects of this pesticide on rat brain tissue can be visualised and explained by  
584 brain oedema, which is an abnormal accumulation of fluid within the brain parenchyma,  
585 producing a volumetric enlargement of the brain cells or tissue (Marmarou, 2007). Indeed,  
586 oedema can lead to increased intracranial pressure, brain herniation, irreversible brain  
587 damage, and ultimately, death. Several factors could be responsible for the induction of  
588 oedema in the brain. The excessive production of free radicals in conjunction with a  
589 weakened scavenger system contributes to both cytotoxic and vasogenic oedema by directly  
590 disrupting the blood brain barrier and by triggering the pathways that mediate brain oedema  
591 (Park, 2004).

592 To further explore the neurotoxicity of Epoxiconazole on the nervous system, we focused our  
593 attention on neural stem cells isolated from the subventricular zone of newborn *Wistar* rats, as  
594 an attractive and robust cell-based *in vitro* model for investigating the possible neurotoxicity  
595 of substances. In particular, we evaluated their potential ability to self-renew, proliferate and  
596 differentiate into neuronal cells during the exposure to sub-chronic EPX. Such NSCs  
597 proliferate and form characteristic primary neurospheres and after their dissociation,  
598 secondary spheres were produced. In this study, EPX treatment clearly inhibited cell viability  
599 and impaired these NSCs proprieties. It reduces the number of neurosphere formation, inhibits  
600 cell proliferation, and perturbs the self-renewal aptitude of NSCs by reducing the number of  
601 secondary neurospheres. In line with our finding, the exposure to Paraquat (herbicide) alone  
602 or in combination with Maneb (fungicide) provoked a significant decrease in cell proliferation  
603 in rat embryonic neural stem cells (Colle et al., 2018). NSC self-renewal and proliferation are  
604 critical for neurogenesis, which is a complicated procedure beginning from the destiny pledge  
605 of neural stem cells and terminating with the differentiation into neurons (Xiong et al., 2019).  
606 The disruption of these proprieties can lead to neurotoxicity. Moreover, NSCs differentiation

607 accompanies and supports the development of the nervous system (Andrieu et al., 2003). In  
608 our investigation, we found that EPX exposure strongly decreased the expression of neural  
609 genes, including Nestin, TUBB3, GFAPa, and CNP, which are respectively correlated to the  
610 proliferation of NSCs, or their differentiation into neurons, astrocytes and oligodendrocytes.  
611 These data indicate that EPX could affect the differentiation of NSCs and thus destruct the  
612 regular growth of the nervous system, which are in accordance with previous report of Huang  
613 et al. (2019) indicating that the exposure to Paraquat strongly affects the differentiation of  
614 human umbilical cord blood-neural stem cells (HUCB-NSCs). As neural stem cells represent  
615 the principal origin of new or renewal neurons (Grade and Gotz, 2017), neural stem cell  
616 disturbance is considered to be a crucial feature of brain damage. Collectively, these data  
617 indicate that pesticides may provoke considerable injury to embryonic NSCs.

618 Accumulating evidence indicated that NSCs are easily affected by oxidative stress (Liomli et  
619 al., 2004; Chang et al., 2013; Li et al., 2019). In our survey, we found that EPX induces  
620 significantly the generation of ROS in a dose-dependent manner. Too much ROS generation  
621 can attack the biological organelles such as the cytoskeleton and mitochondria, and cause  
622 veritable damage to their structure and function. The cytoskeleton, including microtubules,  
623 plays a primordial function in the stability of neural cells. Tubulin immunostaining revealed  
624 that the incubation of NSCs with EPX induces a marked disruption of their microtubule  
625 network. The perturbation of the microtubule organization can lead to the arrest of the cell  
626 cycle as confirmed by the cell proliferation inhibition. ROS also acts as a crucial inducer of  
627 apoptosis (Redza-Dutordoir and Averill-Bates, 2016), and a close relationship exists between  
628 the cytoskeleton degradation and apoptosis. In order to confirm the onset of the programmed  
629 cell death, Annexin V/PI dyes combination was used. Our finding indicated that EPX  
630 increases the rate of apoptosis in a dose-dependent manner. Moreover, mitochondria represent  
631 the principal source and target of oxidative stress. They play a primordial role in the cell  
632 stability as energy producers. The homoeostasis of the mitochondrial dynamics  
633 (fusion/fission) is an important factor for mitochondrial survival. When, the equilibrium is  
634 disturbed, several morphological and functional damages will be produced in mitochondria.  
635 The mitochondrial failure is considered to be a major factor of cell proliferation inhibition and  
636 apoptosis. In this study, in order to investigate the mitochondrial morphology of NSCs, the  
637 MitoTracker Red dye was used. We observed that EPX exposure modified the mitochondrial  
638 morphology from tubular to punctuated structures. In addition, the excessive generation of  
639 ROS induces opening of mitochondrial pores, which can lead to the loss of the mitochondrial

640 membrane potential (Engel and Evens, 2006). Our results showed that EPX-treated NSCs  
641 cells induce the collapse of mitochondrial membrane potential, which is considered to be a  
642 characteristic of the onset of the intrinsic apoptotic pathway. Indeed, the activation of the  
643 effector caspases (caspase-3) is a key feature of the apoptosis execution (Alam et al., 2019).  
644 Our findings suggested that EPX-treated NSCs cells induce the programmed cell death via  
645 caspases dependent signaling pathway. Several studies demonstrated that the proliferative  
646 potential of NSCs is the main determinant of the number of neurons in the brain (Homem et  
647 al., 2015). In pathological conditions like chemical exposures, the NSCs properties disruption  
648 may produce a catastrophic damage to the nervous system increasing the risk of the  
649 neurodegenerative diseases later in life (Landirgan et al., 2005). To our knowledge, there is no  
650 detailed investigation that describes adverse effects associated with agricultural triazole  
651 (Epoiconazole) exposure on neural stem cells *in vivo*. One possibility could be to  
652 administrate locally the chemical in the subventricular area of the brain of rats, and using the  
653 acceptable daily intake as dose of reference (8  $\mu\text{g}/\text{kg}$ ).

654 Taken together, our data show for the first time that the fungicide Epoiconazole can induce  
655 dramatic brain damage *in vivo* and *in vitro* by targeting NSC and impairing their properties.  
656 Also, the excessive ROS production is the principal cause of EPX-induced programmed cell  
657 death probably via the intrinsic pathway. Consequently, the use of this chemical compound  
658 should be promptly limited.

659

660

661 **5. Declarations**

662 **Funding:**

663 This research is supported by INSERM (Institut National de la Santé et de la Recherche  
664 Médicale) and the Ligue contre le Cancer to Joel EYER.

665 **Competing interests**

666 The authors declare that they have no competing interests or personal relationships that could  
667 have appeared to influence the work reported in this paper.

668 **Availability of data and material**

669 All the original data, especially laboratory notebooks, are available on request.

670 **Author contribution**

671 **Hiba HAMDI:** Conceptualization; Investigation; Data curation; Writing original draft.

672 **Imen Graiet:** Experiments.

673 **Salwa ABID-ESSEFI:** Resources; Supervision.

674 **Joel EYER:** Project administration; Supervision; Funding acquisition; Writing and editing.

675 **Ethical approval**

676 The experimental procedures were performed in accordance to the National Institute of Health  
677 Guidelines for Animal Care (Council of European Communities, 1986) and approved by the  
678 local Ethics Committee of Faculty of Pharmacy of Monastir (Ethical number: FPHM/Pro,  
679 201563).

680 **Consent to participate**

681 Not applicable.

682 **Consent for publication**

683 Not applicable.

684 **Acknowledgements**

685 This work is supported by INSERM (Institut National de la Santé et de la Recherche  
686 Médicale) and the Ligue contre le Cancer to Joel EYER. The authors warmly acknowledge

687 Rodolphe Perrot from SCIAM (Service Commun d'Imageries et d'Analyses Microscopiques),  
688 and Catherine Guillet from PACeM (Plateforme d'Analyses Cellulaires et Moléculaires).

689

690

691 **6. References**

- 692  
693 Acuna, L.G., Calderon, I.L., Elias, A.O., Castro, M.E., Vasquez, C.C. Expression of the ygg E  
694 gene protects *Escherichia coli* from potassium tellurite-generated oxidative stress.  
695 *Archives of Microbiology*. 191, 473–476 (2009).
- 696 Aimone, J.B., Li, Y., Lee, S.W., Clemenson, G.D., Deng, W., Gage, F.H. Regulation and  
697 function of adult neurogenesis: from genes to cognition. *Physiological Reviews*. 94,  
698 991–1026 (2014).
- 699 Alam, R.T., Imam, T. S., Abo-Elmaaty, A. M. A., Arisha, A. H. Amelioration of fenitrothion  
700 induced oxidative DNA damage and inactivation of caspase-3 in the brain and spleen  
701 tissues of male rats by N-acetylcysteine. *Life Sciences*. 231, 116534 (2019).
- 702 Aleck, K.A., Bartley, D.L. Multiple malformation syndrome following fluconazole use in  
703 pregnancy: report of an additional patient. *American Journal of Medical Genetics*. 72,  
704 253–256 (1997).
- 705 Altman, J.; Das, G.D. Autoradiographic and histological evidence of postnatal hippocampal  
706 neurogenesis in rats. *Journal of Comparative Neurology*. 124, 319-35 (1965).
- 707 Andrieu, D., Watrin, F., Niinobe, M., Yoshikawa, K., Muscatelli, F., Fernandez, P.A.  
708 Expression of the Prader-Willi gene *Necdin* during mouse nervous system development  
709 correlates with neuronal differentiation and p75NTR expression. *Gene Expression*  
710 *Patterns*. 3, 761-765 (2003).
- 711 Anthony, B., Zhou, F.C., Ogawa, T., Goodlett, C.R., Ruiz, J. Alcohol exposure alters cell  
712 cycle and apoptotic events during early neurulation. *Alcohol Alcohol*. 43, 261–273  
713 (2008).
- 714 Bertelsen, J.R, de Neergaard, E., Smedegaard-Petersen, V. Fungicidal effects of azoxystrobin  
715 and epoxiconazole on phyllosphere fungi, senescence and yield of winter wheat. *Plant*  
716 *Pathology*. 50, 190–205 (2001).
- 717 Bolognesi, C. Genotoxicity of pesticides: a review of a human biomonitoring studies.  
718 *Mutation Research/Reviews in Mutation Research*. 543, 251–272 (2003).
- 719 Bradford, M.M. A rapid and sensitive method for the quantification of microgram quantities  
720 of protein utilizing the principle of protein-dye binding. *Analytical Biochemistry*. 72,  
721 218-254 (1976).
- 722 Chaâbane, M., Ghorbel, I., Elwej, A., Mnif, H., Boudawara, T., Chaâbouni, S. E., Soudani, N.  
723 Penconazole alters redox status, cholinergic function, and membrane-bound ATPases in  
724 the cerebrum and cerebellum of adult rats. *Human & Experimental Toxicology*. 36, 854–  
725 866 (2016).
- 726 Chambers, J.E., Greim, H., Kendall, R.J., Segner, H., Sharpe, R.M., Van Der Kraak,  
727 G. Human and ecological risk assessment of a crop protection chemical: a case study  
728 with the azole fungicide epoxiconazole. *Critical Reviews in Toxicology*. 44, 176–210  
729 (2013).
- 730 Chang, X., Lu, W., Dou, T., Wang, X., Lou, D., Sun, X., Zhou, Z. Paraquat inhibits cell  
731 viability via enhanced oxidative stress and apoptosis in human neural progenitor cells.  
732 *Chemico-Biological Interactions*. 206, 248–255 (2013).
- 733 Colle, D., Farina, M., Ceccatelli, S., Raciti, M. Paraquat and maneb exposure alters rat neural  
734 stem cell proliferation by inducing oxidative stress: new insights on pesticide-induced  
735 neurodevelopmental toxicity. *Neurotoxicity Research*. 34, 820–833 (2018).
- 736 Collins, A.R., Dusinska, M., Gedik, C.M., Stetina, R. Oxidative damage to DNA: do we have  
737 a reliable biomarker? *Environmental Health Perspectives*. 104, 465–469 (1996).

738 Coronas, V., Bantubungi, K., Fombonne, J., Krantic, S., Schiffmann, S.N., Roger, M.  
739 Dopamine D3 receptor stimulation promotes the proliferation of cells derived from the  
740 post-natal subventricular zone. *Journal of Neurochemistry*. 91, 292–1301 (2004).

741 Council of European Communities. 1986. Council instructions about the protection of living  
742 animals used in scientific investigations. *Official Journal of the European Communities*  
743 (JO86/609/CEE). L358, 1–18 (1986).

744 Crofton, K.M. A structure-activity relationship for the neurotoxicity of triazole fungicides.  
745 *Toxicology Letters*. 84, 155–159 (1996).

746 De Castro, V.L, Maia, A.H. Prenatal epoxiconazole exposure effects on rat postnatal  
747 development: birth defects research. *Developmental and Reproductive Toxicology*. 95,  
748 123–9 (2012).

749 EFSA Scientific Report (2008a) Conclusion on the peer review of epoxiconazole, vol 138, pp  
750 1–80

751 EPA. Reregistration Eligibility Decision for Triadimefon and Tolerance Reassessment for  
752 Triadimenol (Washington) (2006).

753 Elhady, A.M., Khalaf, A.A.A., Kamel, M.M., Noshay, P.A. Carvacrol ameliorates behavioral  
754 disturbances and DNA damage in the brain of rats exposed to propiconazole.  
755 *Neurotoxicology*. 70, 19-25 (2019).

756 Ellman, G.L., Courtney, K.D., Andres, V., Feather-Stone, R.M. A new and rapid colorimetric  
757 determination of acetylcholinesterase activity. *Biochemical Pharmacology*. 7, 88–95  
758 (1961).

759 Engel, R.H., and Evens, A.M. 2006. Oxidative stress and apoptosis: a new treatment paradigm  
760 in cancer. *Frontiers. Bioscience*. 11, 300–312 (2016).

761 Eriksson, P.S.; Perfilieva, E.; Bjork-Eriksson, T.; Alborn, A.M.; Nordborg, C.; Peterson,  
762 D.A.; Gage, F.H. Neurogenesis in the adult human hippocampus. *Nature Medicine*. 4,  
763 1313-7 (1998).

764 Flohe, L., Gunzler, W.A. Assays of glutathione peroxidase. *Methods in Enzymology*. 105,  
765 114–121 (1984).

766 Floyd, R.A and Carney, J.M. Free radical damage to protein and DNA: mechanisms involved  
767 and relevant observations on brain undergoing oxidative stress. *Annals of Neurology*.  
768 32: 22–27 (1992).

769 Fuhrman, B., Partoush, A, Aviram, M. Acetylcholine esterase protects LDL against  
770 oxidation. *Biochemical and Biophysical Research Communications*. 322, 974–978  
771 (2004).

772 Gage, F.H., and Temple, S. Neural stem cells: generating and regenerating the brain. *Neuron*.  
773 80, 588–601 (2013).

774 Gao, Q., Gao, Y.M. Hyperglycemic condition disturbs the proliferation and cell death of  
775 neural progenitors in mouse embryonic spinal cord. *International Journal of*  
776 *Developmental Neuroscience*. 25, 349–357 (2007).

777 Giavini, E., and Menegola, E. Are azole fungicides a teratogenic risk for human conceptus?  
778 *Toxicology Letters*. 198, 106–111 (2010).

779 Grace, A.A. Dysregulation of the dopamine system in the pathophysiology of schizophrenia  
780 and depression. *Nature Reviews Neuroscience*. 17, 524–532 (2016).

781 Grade, S., Gotz, M. Neuronal replacement therapy: previous achievements and challenges  
782 ahead. *npj Regenerative Medicine*. 2, 29 (2017).

783 Gu, N., Hu, H., Guo, Q., Jin, S., Wang, C., Oh, Y., Feng, Y., Wu, Q. Effects of oral  
784 administration of titanium dioxide fine-sized particles on plasma glucose in mice. *Food*  
785 *Chem. Toxicol*, 86, 124-131 (2015).

786

787 Habig, W.H., Pabst, M.J., Jakoby, W.B. Glutathione S-transferases, the first enzymatic step in  
788 mercapturic acid formation. *The Journal of Biological Chemistry*. 249, 7130–7139  
789 (1974).

790 Hamdi, H., Abid-Essefi, S., & Eyer, J. Cytotoxic and genotoxic effects of epoxiconazole on  
791 F98 glioma cells. *Chemosphere*. 229, 314-323 (2019a).

792 Hamdi, H., Othmène, Y.B., Ammar, O., Klifi, A., Hallara, E., Ghali, F.B., Abid-Essefi, S.  
793 Oxidative stress, genotoxicity, biochemical and histopathological modifications induced  
794 by epoxiconazole in liver and kidney of Wistar rats. *Environmental Science and  
795 Pollution*. 26, 17535-17547 (2019b).

796 Hamdi, H., Ben Salem, I., Ben Othmène, Y., Annabi, E., & Abid-Essefi, S. The involvement  
797 of ROS generation on Epoxiconazole-induced toxicity in HCT116 cells. *Pesticide  
798 Biochemistry and Physiology*. 148, 62–67 (2018).

799 Hattab, S., Boughattas, I., Boussetta, H., Viarengo, A., Banni, M., Sforzini, S. Transcriptional  
800 expression levels and biochemical markers of oxidative stress in the earthworm  
801 *Eisenia andrei* after exposure to 2,4-dichlorophenoxyacetic acid (2,4-D). *Ecotoxicology  
802 and Environmental Safety*. 122, 76–82 (2015).

803 Heusinkveld, H.J., Molendijk, J., Van den Berg, M., Westerink, R.H.S. Azole fungicides  
804 disturb intracellular  $Ca^{2+}$  in an additive manner in dopaminergic PC12 cells.  
805 *Toxicological Science*. 134, 374–381 (2013).

806 Homem, C.C., Repic, M., Knoblich, J.A. Proliferation control in neural stem and progenitor  
807 cells. *Nature Reviews Neuroscience*. 16, 647–659 (2015).

808 Huang, M., Cai, Q., Xu, Y., Guo, M., Zhu, C., Li, Y., Yang, H. Paraquat affects the  
809 differentiation of neural stem cells and impairs the function of vascular endothelial cells:  
810 a study of molecular mechanism. *Environmental Toxicology*. 34, 548-555 (2019).

811 Khacho, M., Clark, A., Svoboda, D.S., Azzi, J., MacLaurin, J., Meghaizel, C., Sesaki, H.,  
812 Lagace, D.C., Germain, M., Harper, M.E., Park, D.S., Slack, R.S. Mitochondrial  
813 dynamics impacts stem cell identity and fate decisions by regulating a nuclear  
814 transcriptional program. *Cell Stem Cell*. 19, 232–247 (2016).

815 Kukekov, V.G.; Laywell, E.D.; Suslov, O.; Davies, K.; Scheffler, B.; Thomas, L.B.; O'Brien,  
816 T.F.; Kusakabe, M.; Steindler, D.A. Multipotent stem/progenitor cells with similar  
817 properties arise from two neurogenic regions of adult human brain. *Experimental  
818 Neurology*. 156, 333-44 (1999).

819 Landrigan, P.J., Sonawane, B., Butler, R.N., Trasande, L., Callan, R., Droller, D. Early  
820 environmental origins of neurodegenerative disease in later life. *Environmental Health  
821 Perspectives*. 113, 1230–1233 (2005).

822 Le Belle, J.E., Orozco, N.M., Paucar, A.A., Saxe, J.P., Mottahedeh, J., Pyle, A.D., Kornblum,  
823 H.I. Proliferative neural stem cells have high endogenous ROS levels that regulate  
824 self-renewal and neurogenesis in a PI3K/Akt-dependant manner. *Cell Stem Cell*. 8, 59–  
825 71 (2011).

826 Lépinoux-Chambaud, C., Barreau, K., & Eyer, J. The Neurofilament-Derived Peptide NFL-  
827 TBS.40-63 Targets Neural Stem Cells and Affects Their Properties. *Stem Cells  
828 Translational Medicine*. 5, 901-913 (2016).

829 Li, Q., Wang, P., Huang, C., Chen, B., Liu, J., Zhao, M., & Zhao, J. N-Acetyl serotonin  
830 protects neural progenitor cells against oxidative stress-induced apoptosis and improves  
831 neurogenesis in adult mouse hippocampus following traumatic brain injury. *Journal of  
832 Molecular Neuroscience*. 67, 574–588 (2019).

833 Limoli, C.L., Giedzinski, E., Rola, R., Otsuka, S., Palmer, T.D., Fike, J.R. Radiation response  
834 of neural precursor cells: linking cellular sensitivity to cell cycle checkpoints, apoptosis  
835 and oxidative stress. *Radiation Research*. 161, 17–27 (2004).

836 Lin, M.T., Beal, M.F. Mitochondrial dysfunction and oxidative stress in neurodegenerative  
837 diseases. *Nature*. 443, 787–795 (2006).

838 Loh, K.P., Huang, S.H., De Silva, R., Tan, B.K., and Zhu, Y.Z. Oxidative stress: apoptosis in  
839 neuronal injury. *Current Alzheimer Research*. 3, 327–337 (2006).

840 Marmarou A. A review of progress in understanding the pathophysiology and treatment of  
841 brain edema. *Neurosurg Focus* 2007; 22: 1323–1329.

842 Marklund, S., Marklund, G. Involvement of the superoxide anion radical in the autoxidation  
843 of pyrogallol and a convenient assay for superoxide dismutase. *European Journal of*  
844 *Biochemistry*. 47, 469–474 (1974).

845 Menegola, E., Broccia, M.L., Di Renzo, F., Massa, V., and Giavini, E. Study on the common  
846 teratogenic pathway elicited by the fungicides triazole-derivatives. *Toxicology in*  
847 *Vitro*. 19, 737–748 (2005).

848 Mercier, Y., Gatellier, P., Renerre, M. Lipid and protein oxidation in vitro, and antioxidant  
849 potential in meat from Charolais cows finished on pasture or mixed diet. *Meat Science*.  
850 66, 467–473 (2004).

851 Moreno, M.C.R., Fussell, K.C., Groeters, S., Schneider, S., Strauss, V., Stinchcombe, S.,  
852 Fegert, I., Veras, M., van Ravenzwaay, B. Epoxiconazole-induced degeneration in rat  
853 placenta and the effects of estradiol supplementation. *Birth Defects Research Part B*. 98,  
854 208–21 (2013).

855 Mouisel E, Blondet B, Escourrou P, et al. Outcome of acetylcholinesterase deficiency for  
856 neuromuscular functioning. *Neurosci Res* 2006; 55: 389–96.

857 Murphy, M.P. Mitochondrial dysfunction indirectly elevates ROS production by the  
858 endoplasmic reticulum. *Cell Metabolism*. 18, 145–146 (2013).

859 Narra, M.R, Rajender, K., Reddy, R.R., Murty, U.S., Begum, G. Insecticides induced stress  
860 response and recuperation in fish: biomarkers in blood and tissues related to oxidative  
861 damage. *Chemosphere*. 168, 350–357 (2017).

862 Nicoleau, C., Benzakour, O., Agasse, F., Thiriet, N., Petit, J., Prestoz, L., Roger, M., Jaber,  
863 M., Coronas, V. Endogenous hepatocyte growth factor is a niche signal for  
864 subventricular zone neural stem cell amplification and self-renewal. *Stem Cells*. 27,  
865 408–419 (2009).

866 Nieradko-Iwanicka, B., Borzecki, A. Subacute poisoning of mice with deltamethrin produces  
867 memory impairment reduced locomotor activity, liver damage and changes in blood  
868 morphology in the mechanism of oxidative stress. *Pharmacological Reports*. 67, 535–  
869 541 (2015).

870 Ohkawa, H., Ohishi, N., Yagi, K. Assay for lipid peroxide in animal tissues by thiobarbituric  
871 acid reaction. *Analytical Biochemistry*. 95, 351–358 (1979).

872 Passeport, E., Benoit, P., Bergheaud, V., Coquet, Y., Tournebize, J. Epoxiconazole  
873 degradation from artificial wetland and forest buffer substrates under flooded conditions.  
874 *Chemical Engineering*, 173, 760–765 (2011).

875 Park, S, Yamaguchi, M, Zhou, C, et al. Neurovascular protection reduces early brain injury  
876 after subarachnoid hemorrhage. *Stroke*; 35: 2412–2417 (2004).

877 Pearson, B.L., Simon, J.M., McCoy E.S., Salazar, G., Fragola, G., Zylka, M.J. Identification  
878 of chemicals that mimic transcriptional changes associated with autism, brain aging and  
879 neurodegeneration. *Nature Communications*. 7, 1–12 (2016).

880 Pencea, V.; Bingaman, K.D.; Freedman, L.J.; Luskin, M.B. Neurogenesis in the  
881 subventricular zone and rostral migratory stream of the neonatal and adult primate  
882 forebrain. *Experimental Neurology*. 172, 1-16 (2001).

883 Perez Estrada, C., Covacu, R., Sankavaram, S.R., Svensson, M., Brundin, L. Oxidative stress  
884 increases neurogenesis and oligodendrogenesis in adult neural progenitor cells. *Stem*  
885 *Cells and Development*. 23, 2311–2327 (2014).

886 Redza-Dutordoir, M., and Averill-Bates, D. A. Activation of apoptosis signalling pathways by  
887 reactive oxygen species. *Biochimica Biophysica Acta*. 1863, 2977–2992.

888 Robbins SL and Angel LD. Basic pathology. 2nd ed. Philadelphia, London: WB Saunders  
889 Co, (1976).

890 Sayre, L.M., Perry, G, and Smith, M.A. Oxidative Stress and Neurotoxicity. *Chem. Res.*  
891 *Toxicol.* 21, 172–188 (2008).

892 Schwarzbacherová, V., Wnuk, M., Lewinska, A., Potocki, L., Zebrowski, J., Kozirowski,  
893 M., Dianovský, J. Evaluation of cytotoxic and genotoxic activity of fungicide  
894 formulation Tango® .Super in bovine lymphocytes. *Environmental Pollution*. 220, 255–  
895 263 (2017).

896 Silman, I., Sussman, J.L. Acetylcholinesterase: Bclassical and Bnonclassical functions and  
897 pharmacology. *Current Opinion in Pharmacology*. 5, 293–302 (2005).

898 Stinchcombe, S., Schneider, S., Fegert, I., Rey Moreno, M.C., Strauss, V., Gröters, S., Fabian,  
899 E., Fussell, K.C., Pigott, G.H., van Ravenzwaay, B. Effects of estrogen coadministration  
900 on epoxiconazole toxicity in rats. *Birth Defects Research Part B*. 98, 247–59 (2013).

901 Tabassum, H., Khan, J., Salman, M., Raisuddin, S., Parvez, S. Propiconazole induced  
902 toxicological alterations in brain of freshwater fish *Channapunctata* Bloch. *Ecological*  
903 *Indicators*. 62, 242–248 (2016).

904 Taxvig, C., Hass, U., Axelstad, M., Dalgaard, M., Boberg, J., Andersen, H.R., Vinggaard, A.  
905 Endocrinedisrupting activities in vivo of the fungicides tebuconazole and epoxiconazole.  
906 *Toxicological Science*. 100, 464–73 (2007).

907 Taxvig, C., Vinggaard, A.M., Hass, U., Axelstad, M.,Metzdorff, S., Nellemann, C. Endocrine-  
908 disrupting properties in vivo of widely used azole fungicides. *International Journal of*  
909 *Andrology*. 31, 70–6 (2008).

910 Tincer, G., Mashkaryan, V., Bhattarai, P., & Kizil, C. Neural stem/ progenitor cells in  
911 Alzheimer’s disease. *Yale Journal of Biology and Medicine*. 89, 23–35 (2016).

912 Tsuda, S., Kosaka, Y., Matsusaka, N., Sasaki, Y.F. Detection of pyrimethamine-induced DNA  
913 damage in mouse embryo and maternal organs by the modified alkaline single cell gel  
914 electrophoresis assay. *Mutation Research*. 415, 69–77 (1998).

915 Valadas, J., Mocelin, R., Sachett, A., Marcon, M., Zanette, R. A., Dallegrave, E., Piato, A.  
916 Propiconazole induces abnormal behavior and oxidative stress in zebrafish.  
917 *Environmental Science and Pollution Research*. 26, 27808-27815 (2019).

918 Volkow, N.D., Wise, R.A., Baler, R. The dopamine motive system: implications for drug and  
919 food addiction. *Nature Reviews Neuroscience*. 18, 741–752 (2017).

920 Wang, J. L., Wang, J.J., Cai, Z.N., & Xu, C.J. The effect of curcumin on the differentiation,  
921 apoptosis and cell cycle of neural stem cells is mediated through inhibiting autophagy by  
922 the modulation of Atg7 and p62. *International Journal of Molecular Medicine*, 42, 2481–  
923 2488 (2018).

924 Worek, F., Reiter, G., Eyer, P., Szinicz, L. Reactivation Kinetics of acetylcholinesterase from  
925 different species inhibited by highly toxic organophosphates . *Arch Toxicol*, 76,523-9  
926 (2002).

927 Xin, L., Qiuxu, Y., Ping, Z., Honghua, B. Market situation of epoxiconazole fungicide.  
928 *Agrochemicals*. 49, 790–791 (2010).

929 Xiong, G., Zhao, L., Yan, M., Wang, X., Zhou, Z., Chang, X. N-acetylcysteine Alleviated  
930 Paraquat-Induced Mitochondrial Fragmentation and Autophagy in Primary Murine  
931 Neural Progenitor Cells. *Journal of Applied Toxicology*. 39, 1557-1567 (2019).

932 Zarn, J.A., Brüsweiler, B.J., and Schlatter, J.R. Azole fungicides affect mammalian  
933 steroidogenesis by inhibiting sterol 14 alpha-demethylase and aromatase. *Environmental*  
934 *Health Perspectives*. 111, 255–261 (2003).

935

936 **7. Figure legends**

937 **Fig. 1. Evaluation of absolute and relative brain weights and oxidative stress biomarkers**  
938 **(MDA, PC and DNA damage) of control and Epoxiconazole-treated rats.**

939 (A) Absolute and relative brain weight of rat brains after 28 days of EPX administration at  
940 different doses. Values represent the means  $\pm$  SD.

941 (B) Lipid peroxidation induced in brain tissue after EPX intoxication for 28 days at different  
942 concentrations: 8, 24, 40, and 56 mg/kg bw. Values represent the means  $\pm$  SD.

943 (C) Determination of protein carbonyl level in the brain of *Wistar* rats after EPX treatment.  
944 Values represent the means  $\pm$  SD.

945 (D) Score of DNA damage in brain tissue after EPX administration. Values represent means  $\pm$   
946 SD.

947 **Fig. 2. Enzymatic antioxidant status in the brain of control and Epoxiconazole-treated**  
948 **rats.**

949 Each experiment was repeated 3 times under different treatment conditions and data are  
950 expressed as the mean  $\pm$  SD.

951 (A) Evaluation of CAT activity in the brain of male rats after EPX exposure.

952 (B) Evaluation of SOD activity in the brain after EPX exposure.

953 (C) Measurement of GPx activity in the brain after EPX exposure.

954 (D) Measurement of GST activity in the brain after EPX exposure.

955 **Fig. 3. Cholinergic function and histopathological examination in the brain of control**  
956 **and Epoxiconazole-treated rats.**

957 (A) Evaluation of Acetylcholinesterase (AChE) activity in the brain of *Wistar* rats after EPX  
958 administration. Values represent means  $\pm$  SD.

959 (B) Microscopic evaluation of rat cerebral cortex after EPX treatment, stained with  
960 hematoxylin–eosin (H&E) ( $\times 400$ ). In the control group, the cerebral cortex showed regular  
961 histo-architecture (1, 2 and 3). The damage in cerebral cortex sections (4–9) provoked by  
962 EPX significantly increases. The arrows indicate vacuolated neurons (4), degeneration of

963 Purkinje cells (5 and 6), an inflammation and oedema (7), and dilations of blood vessels and  
964 hemorrhage (8 and 9). ML: molecular layer; PCL: Purkinje cells' layer.

965 **Fig. 4. Effects of the Epoxiconazole fungicide on neural stem cell properties.**

966 (A) Neural stem cells were exposed to EPX at different doses. Results are given as a  
967 percentage of controls (set to 100%). Cell viability was determined using the trypan blue  
968 exclusion technique. Each experiment was repeated 3 times.

969 (B) Morphological evaluation of neurospheres after EPX treatment without or with (2, 5 and  
970 10  $\mu$ M). Scale bars = 400  $\mu$ M.

971 (C) Counting of Primary neurospheres after treatment of NSCs with EPX or colchicine  
972 (5 $\mu$ g/ml). Each experiment was done 3 times. Values represent the means  $\pm$  SD.

973 (D) Evaluation of NSCs ability to self-renew by counting the numbers of secondary  
974 neurospheres.

975 Each experiment was repeated 3 times under different treatment conditions and data are  
976 expressed as the mean  $\pm$  SD.

977 **Fig. 5. Effects of Epoxiconazole on proliferation, differentiation, ROS generation and**  
978 **cytoskeleton organization of rat neural stem cells.**

979 NSCs were treated with EPX (2, 5 and 10  $\mu$ M respectively). Each experiment was repeated at  
980 least 3 times under different treatment conditions and data are expressed as the mean  $\pm$  SD.

981 (A) The percentages of neural stem cells (NSCs) at G1, S, or G2/M phases of the cell cycle  
982 after treatment with increasing concentrations of the EPX.

983 (B) qRT-PCR analysis of the relative gene expression of NESTIN, GFAPa, TUBB3 and CNP  
984 in NSCs after treatment with or without EPX.

985 (C) The oxidation of DCFH to DCF reflects the amount of ROS produced.

986 (D) Microscopic examination using confocal microscopy shows aggregation of microtubules  
987 (MTs), following EPX treatment. Cells treated with EPX at the indicated concentrations (2, 5  
988 and 10  $\mu$ M) have lost their normal microtubule network.

989 **Fig. 6. Epoxiconazole induces mitochondria fragmentation and affects their functions. It**  
990 **also induces apoptosis on neural stem cells via caspases dependent signaling pathway.**

991 (A) MitoTracker fluorescence staining showed that EPX induces mitochondrial  
992 fragmentation.

993 (B) EPX induces depolarization of mitochondria. Treatment of neural stem cells with EPX for  
994 24 h reduced the mitochondrial potential.

995 (C) The apoptosis was detected by Annexin-V/PI double-staining after EPX treatment for 24  
996 h. Each experiment was repeated 3 times. The rate of apoptosis on neural stem cells was  
997 assessed as means  $\pm$  SD.

998 (D) EPX-induced caspase-3 activation on neural stem cells after 24 hours of exposure.

999 Each experiment was repeated 3 times under different treatment conditions and data are  
1000 expressed as the mean  $\pm$  SD.

1001 **Fig. 7. EPX induces neural stem cells properties disruption and programmed cell death**  
1002 **through ROS generation.**

1003 Neural stem cells were pre-treated for 2 h with 1 mM N-acetylcysteine (NAC) before adding  
1004 EPX at 10  $\mu$ M for 24 h.

1005 (A) cell viability was quantified using the Trypan blue exclusion technique.

1006 (B and C) The number of primary and secondary neurospheres were counted to evaluate the  
1007 formation and the self-renewal of NSCs.

1008 (D) Evaluation of the mitochondrial transmembrane potential ( $\Delta\psi_m$ ) using Rh-123.

1009 (E) The rate of ROS was examined using DCFH-DA.

1010 (F) The level of apoptosis was analyzed using flow cytometry. Each experiment was repeated  
1011 3 times under different treatment conditions and data are expressed as the mean  $\pm$  SD. \*\*\*P <  
1012 0.001 versus control. ##p < 0.05, ###p < 0.001 versus cells treated with EPX.

**Table 1. Scoring of the histopathological alterations in the brain of rats, treated with different concentrations of EPX.**

(-) none, (+) mild, (++) moderate, (+++) severe.

## Figure legends

### **Fig. 1. Evaluation of absolute and relative brain weights and oxidative stress biomarkers (MDA, PC and DNA damage) of control and Epoxiconazole-treated rats.**

(A) Absolute and relative brain weight of rat brains after 28 days of EPX administration at different doses.

(B) Lipid peroxidation induced in brain tissue after EPX intoxication for 28 days at different concentrations: 8, 24, 40, and 56 mg/kg bw.

(C) Determination of protein carbonyl level in the brain of *Wistar* rats after EPX treatment.

(D) Score of DNA damage in brain tissue after EPX administration.

These different experiments were repeated at least 3 times. Values represent the means  $\pm$  SD, and are significantly different from control (\*P < 0.05; \*\*P < 0.001; \*\*\*P < 0.0001).

### **Fig. 2. Enzymatic antioxidant status in the brain of control and Epoxiconazole-treated rats.**

Each experiment was repeated at least 3 times under different treatment conditions and data are expressed as the mean  $\pm$  SD, (\*P < 0.05; \*\*P < 0.001; \*\*\*P < 0.0001 versus control).

(A) Evaluation of CAT activity in the brain of male rats after EPX exposure.

(B) Evaluation of SOD activity in the brain after EPX exposure.

(C) Measurement of GPx activity in the brain after EPX exposure.

(D) Measurement of GST activity in the brain after EPX exposure.

### **Fig. 3. Cholinergic function and histopathological examination in the brain of control and Epoxiconazole-treated rats.**

(A) Evaluation of Acetylcholinesterase (AChE) activity in the brain of *Wistar* rats after EPX administration. Values represent means  $\pm$  SD.

(B) Microscopic evaluation of rat cerebral cortex after EPX treatment, stained with hematoxylin–eosin (H&E) ( $\times$ 400). In the control group, the cerebral cortex showed regular histo-architecture (1, 2 and 3). The damage in cerebral cortex sections (4–9) provoked by

EPX significantly increases. The arrows indicate vacuolated neurons (4), degeneration of Purkinje cells (5 and 6), an inflammation and oedema (7), and dilations of blood vessels and hemorrhage (8 and 9). ML: molecular layer; PCL: Purkinje cells' layer.

**Fig. 4. Effects of the Epoxiconazole fungicide on neural stem cell properties.**

(A) Neural stem cells were exposed to EPX at different doses. Results are given as a percentage of controls (set to 100%). Cell viability was determined using the trypan blue exclusion technique.

(B) Morphological evaluation of neurospheres after EPX treatment without or with (2, 5 and 10  $\mu$ M). Scale bars = 400  $\mu$ M.

(C) Counting of primary neurosphere formation after treatment of NSCs with EPX or colchicine (5 $\mu$ g/ml).

(D) Evaluation of NSCs ability to self-renew by counting the numbers of secondary neurospheres.

Each complete experiment was repeated at least 3 times under different treatment conditions and data are expressed as the mean  $\pm$  SD. (\*P < 0.05; \*\*P < 0.001; \*\*\*P < 0.0001 versus control cells).

**Fig. 5. Effects of Epoxiconazole on proliferation, differentiation, ROS generation and cytoskeleton organization of rat neural stem cells.**

NSCs were treated with EPX (2, 5 and 10  $\mu$ M respectively). Each full experiment was repeated at least 3 times under different treatment conditions and data are expressed as the mean  $\pm$  SD; \*P < 0.05; \*\*P < 0.001; \*\*\*P < 0.0001 versus control cells.

(A) The percentages of neural stem cells (NSCs) at G1, S, or G2/M phases of the cell cycle after treatment with increasing concentrations of the EPX.

(B) qRT-PCR analysis of the relative gene expression of NESTIN, GFAP $\alpha$ , TUBB3 and CNP in NSCs after treatment with or without EPX.

(C) The oxidation of DCFH to DCF reflects the amount of ROS produced.

(D) Microscopic examination using confocal microscopy shows aggregation of microtubules (MTs), following EPX treatment. Cells treated with EPX at the indicated concentrations (2, 5 and 10  $\mu$ M) have lost their normal microtubule network.

**Fig. 6. Epoxiconazole induces mitochondria fragmentation and affects their functions. It also induces apoptosis on neural stem cells via caspases dependent signaling pathway.**

(A) MitoTracker fluorescence staining showed that EPX induces mitochondrial fragmentation.

(B) EPX induces depolarization of mitochondria. Treatment of neural stem cells with EPX for 24 h reduced the mitochondrial potential.

(C) The apoptosis was detected by Annexin-V/PI double-staining after EPX treatment for 24 h. Each experiment was repeated 3 times. The rate of apoptosis on neural stem cells was assessed as means  $\pm$  SD.

(D) EPX-induced caspase-3 activation on neural stem cells after 24 hours of exposure.

Each experiment was repeated at least 3 times under different treatment conditions and data are expressed as the mean  $\pm$  SD. \*P < 0.05; \*\*P < 0.001; \*\*\*P < 0.0001 versus control cells.

**Fig. 7. EPX induces neural stem cells properties disruption and programmed cell death through ROS generation.**

Neural stem cells were pre-treated for 2 h with 1 mM N-acetylcysteine (NAC) before adding EPX at 10  $\mu$ M for 24 h.

(A) cell viability was quantified using the Trypan blue exclusion technique.

(B and C) The number of primary and secondary neurospheres were counted to evaluate the formation and the self-renewal of NSCs.

(D) Evaluation of the mitochondrial transmembrane potential ( $\Delta\psi_m$ ) using Rh-123.

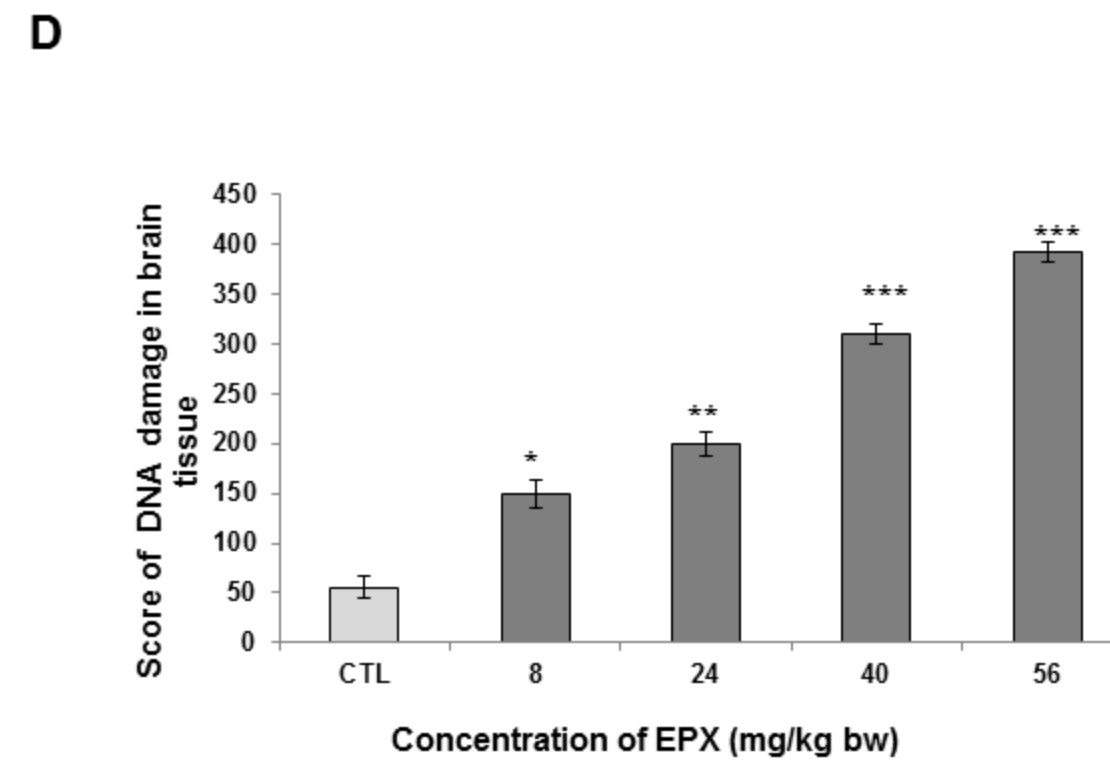
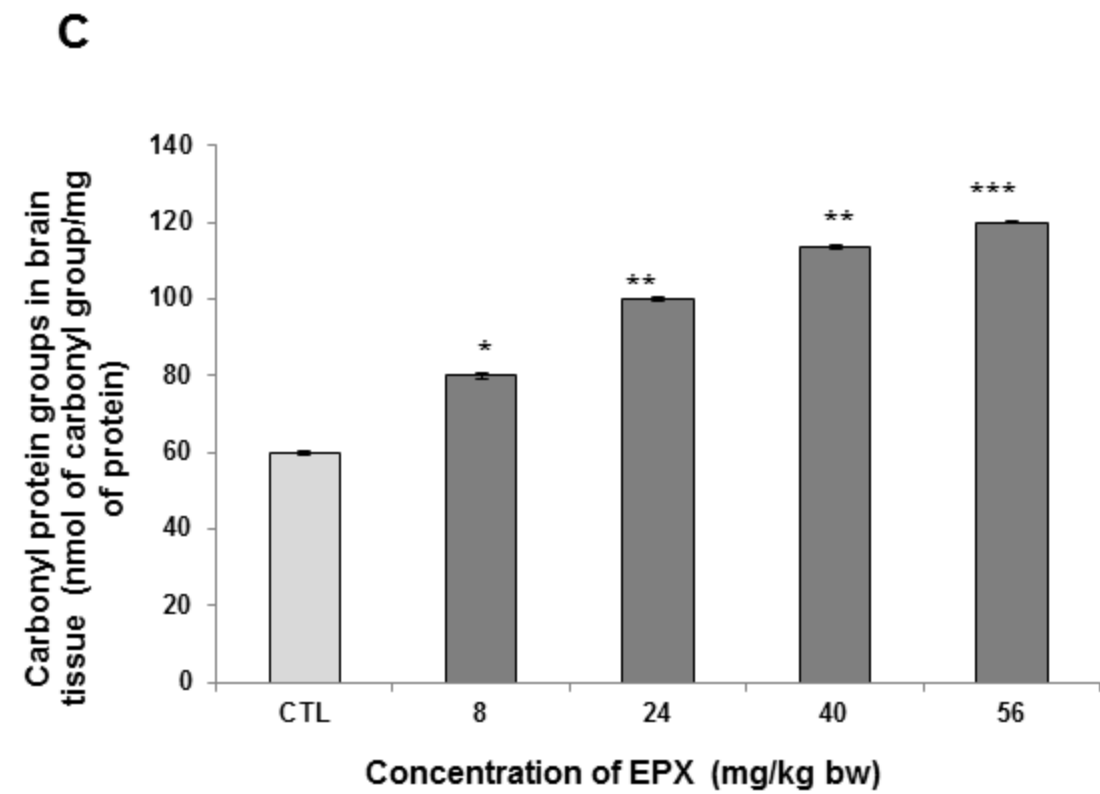
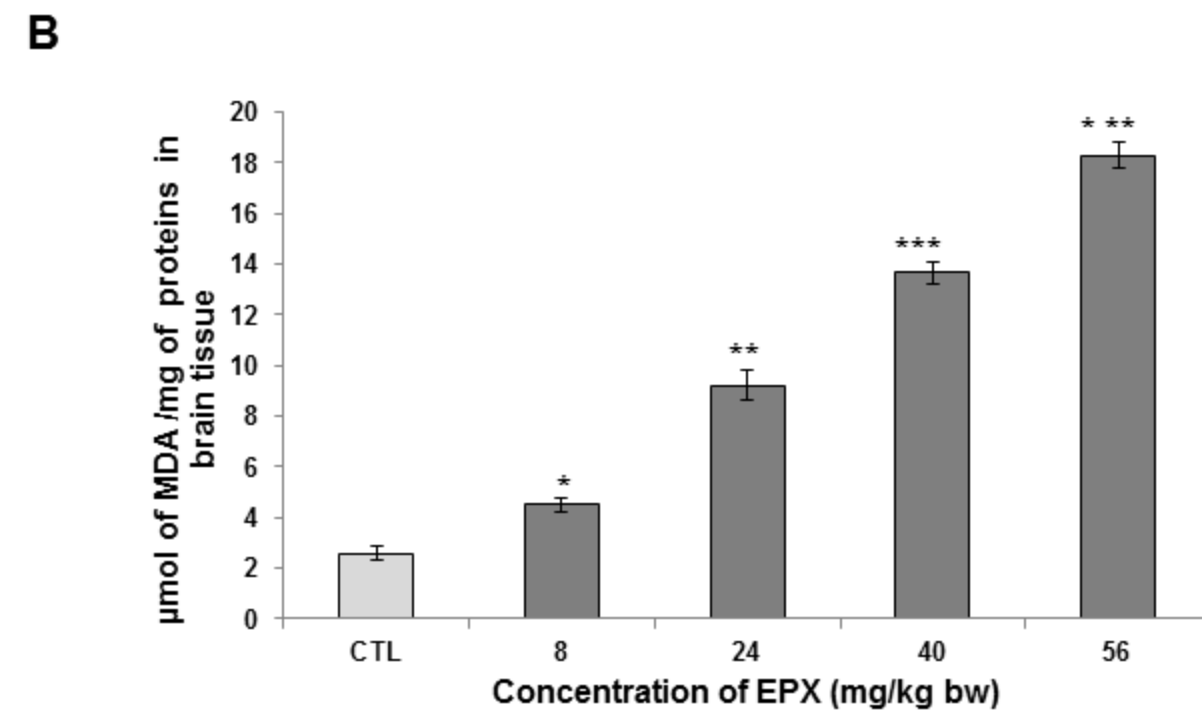
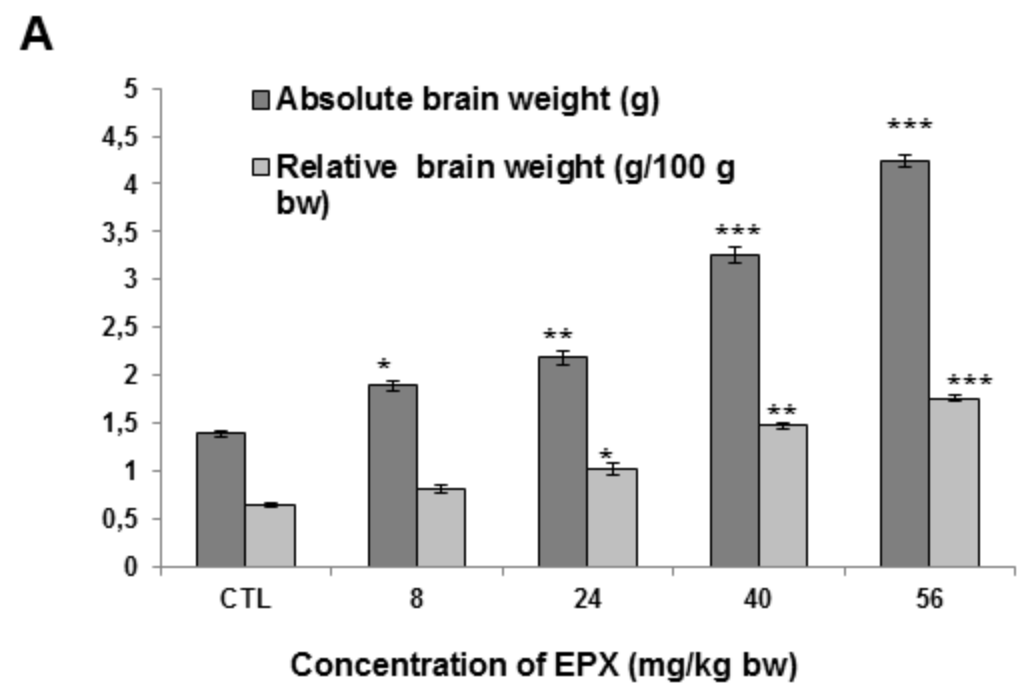
(E) The rate of ROS was examined using DCFH-DA.

(F) The level of apoptosis was analyzed using flow cytometry.

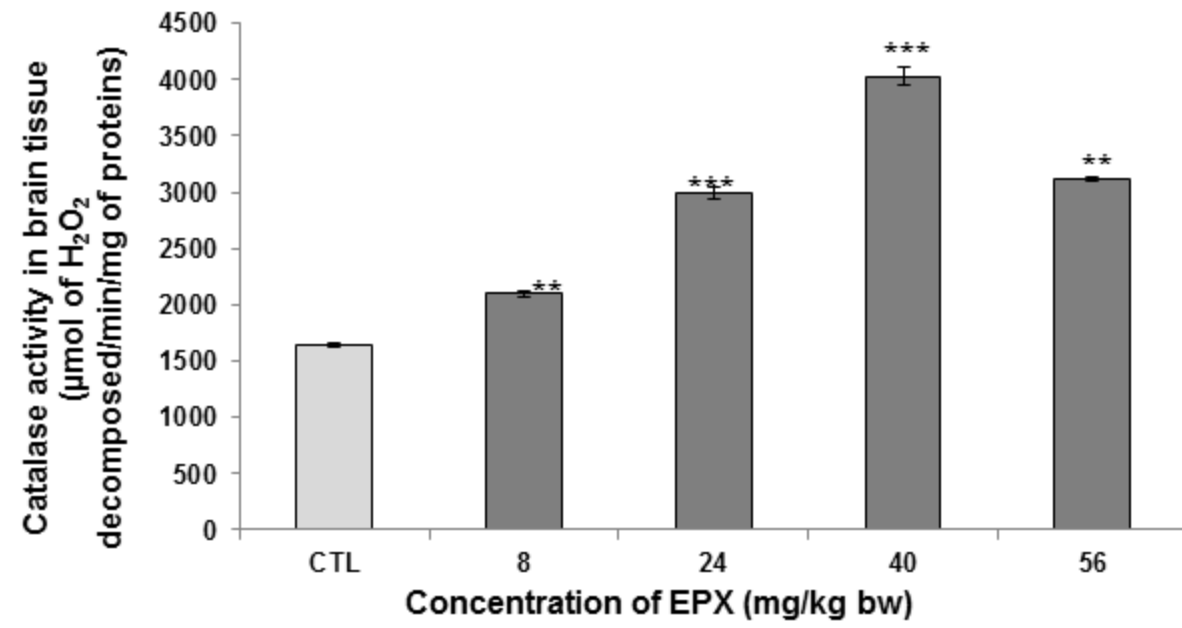
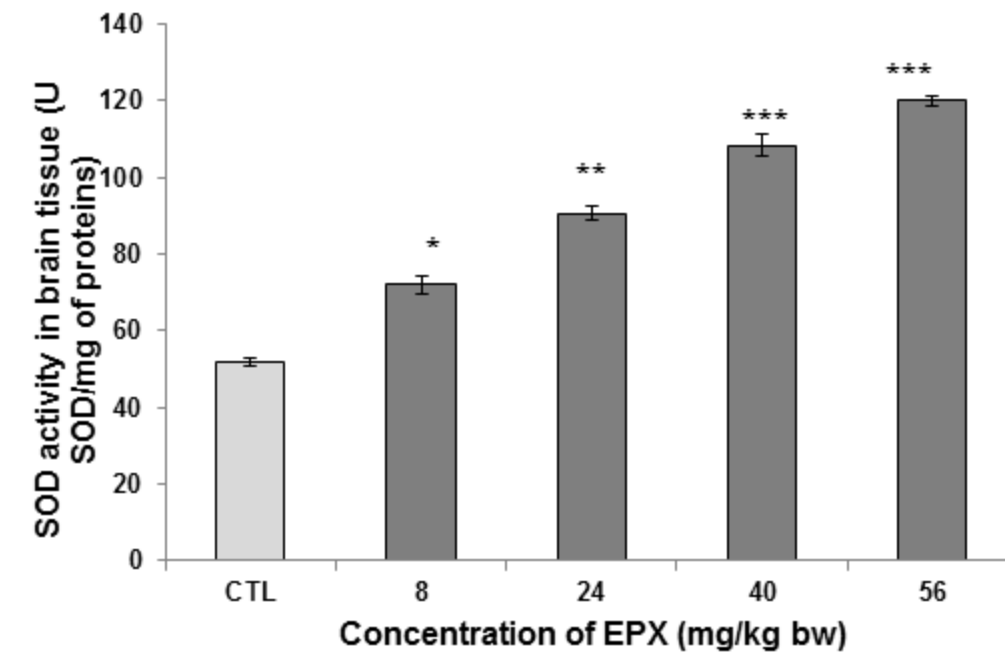
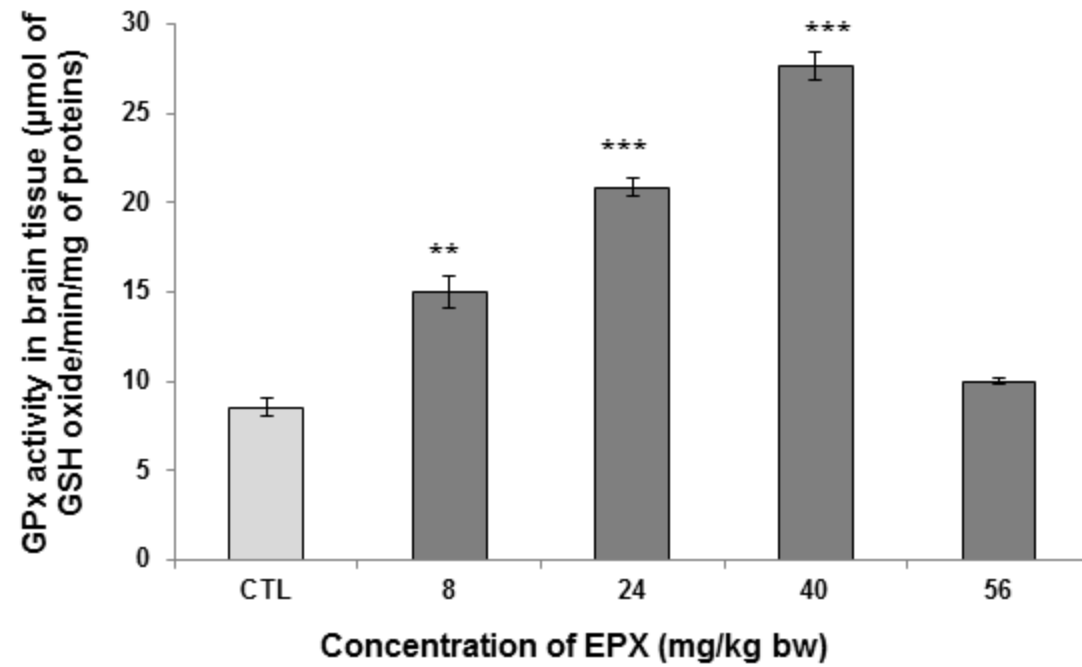
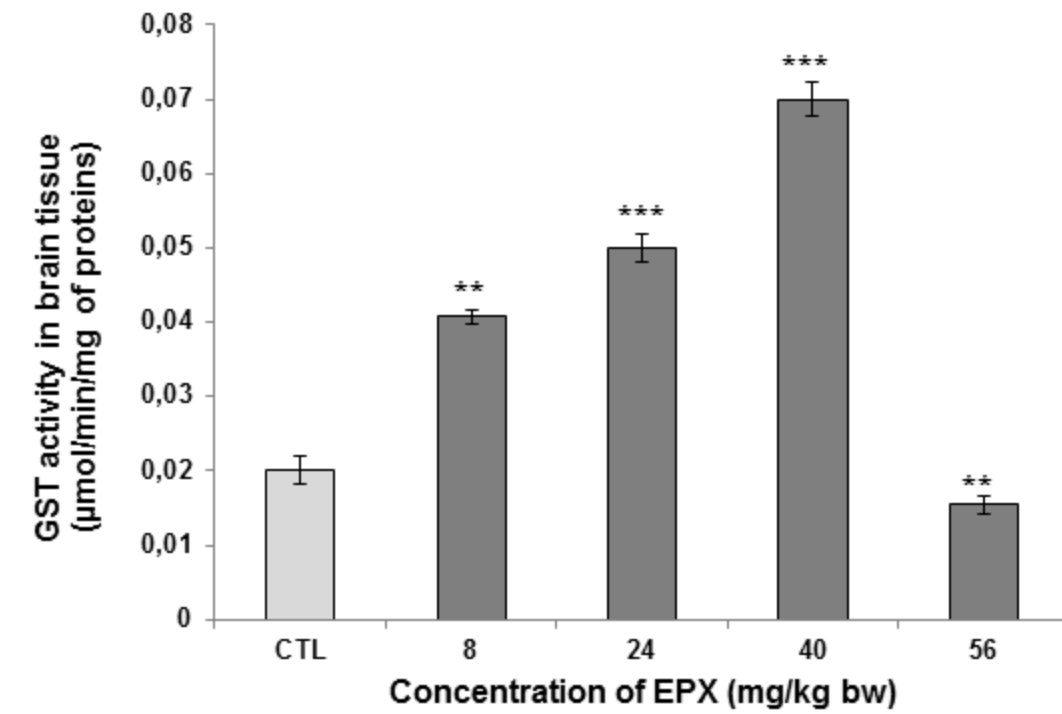
Each experiment was repeated 3 times under different treatment conditions and data are expressed as the mean  $\pm$  SD. \*\*\*P < 0.001 versus control. ##p < 0.05, ###p < 0.001 versus cells treated with EPX.

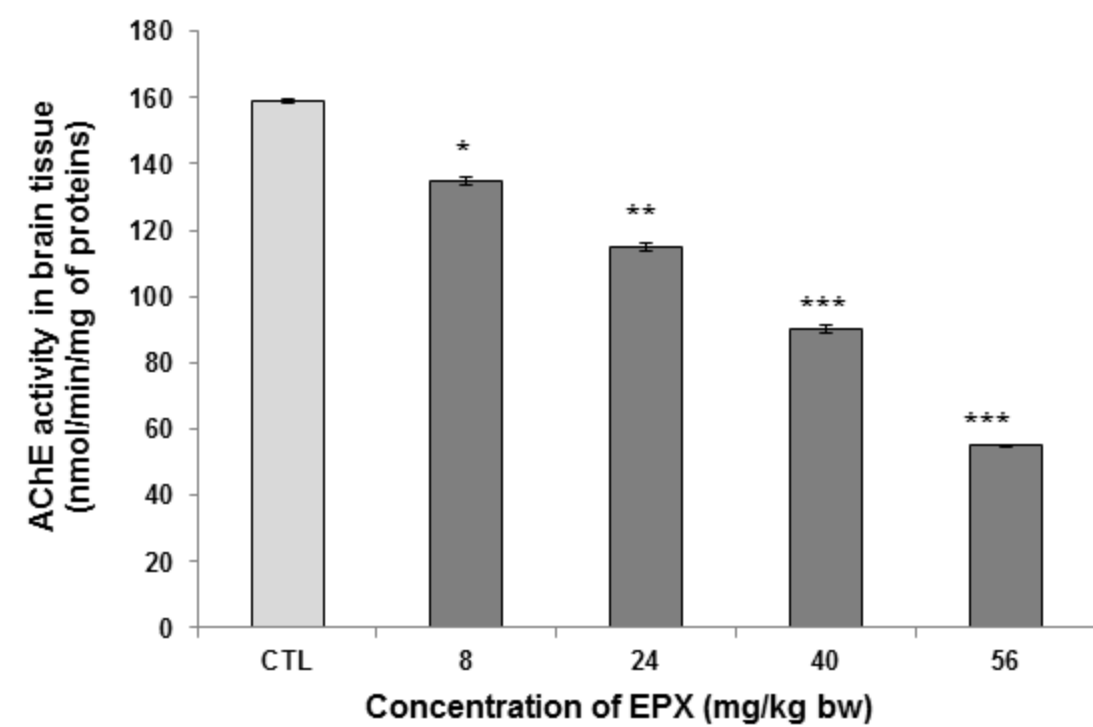
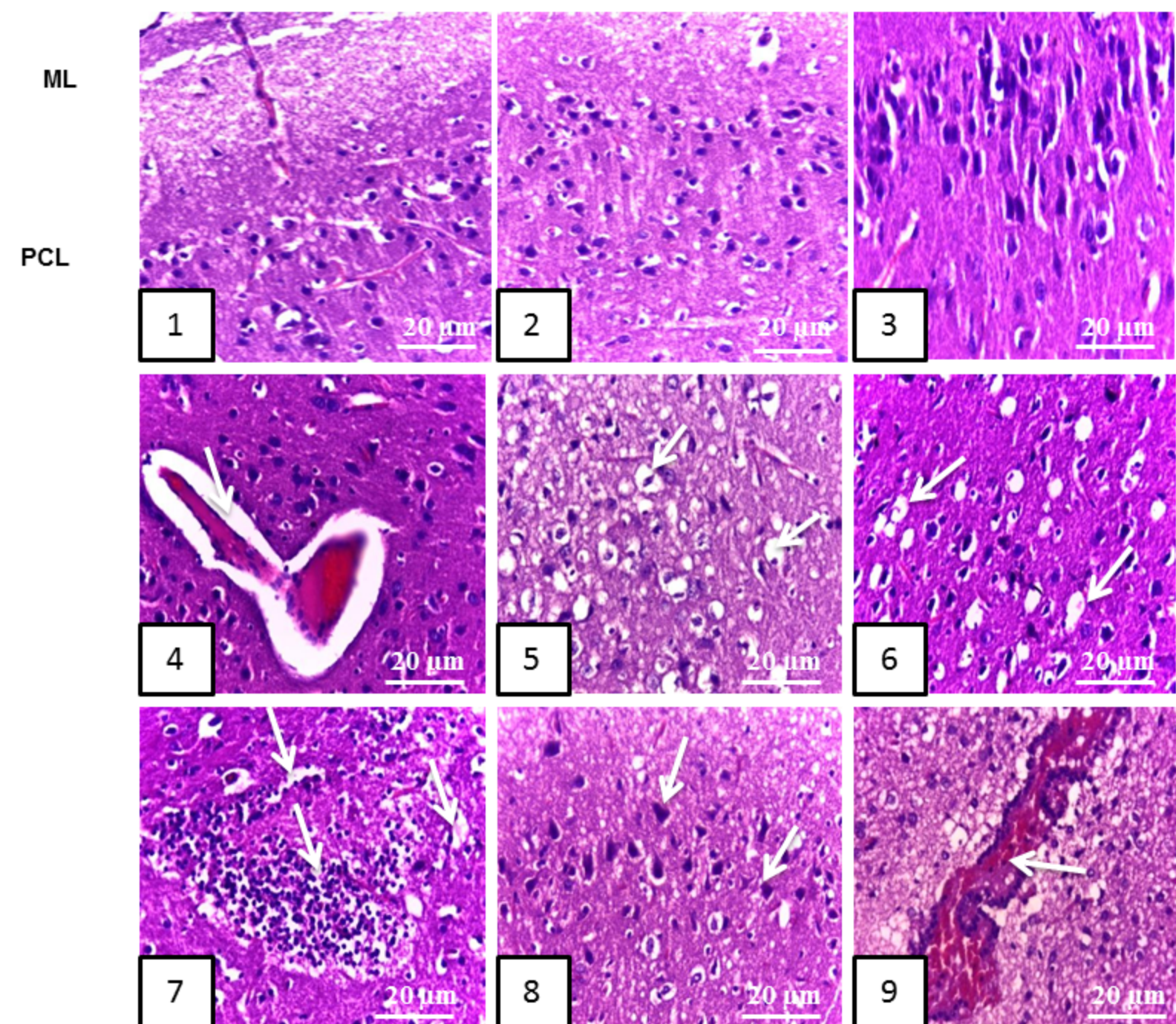
**Table 1. Scoring of the histopathological alterations in the brain of rats, treated with different concentrations of EPX.**

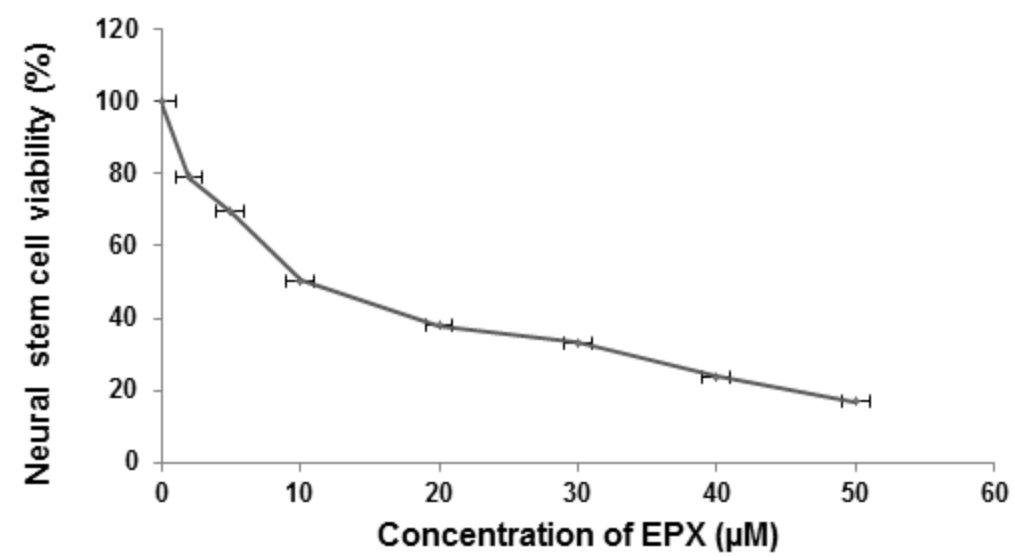
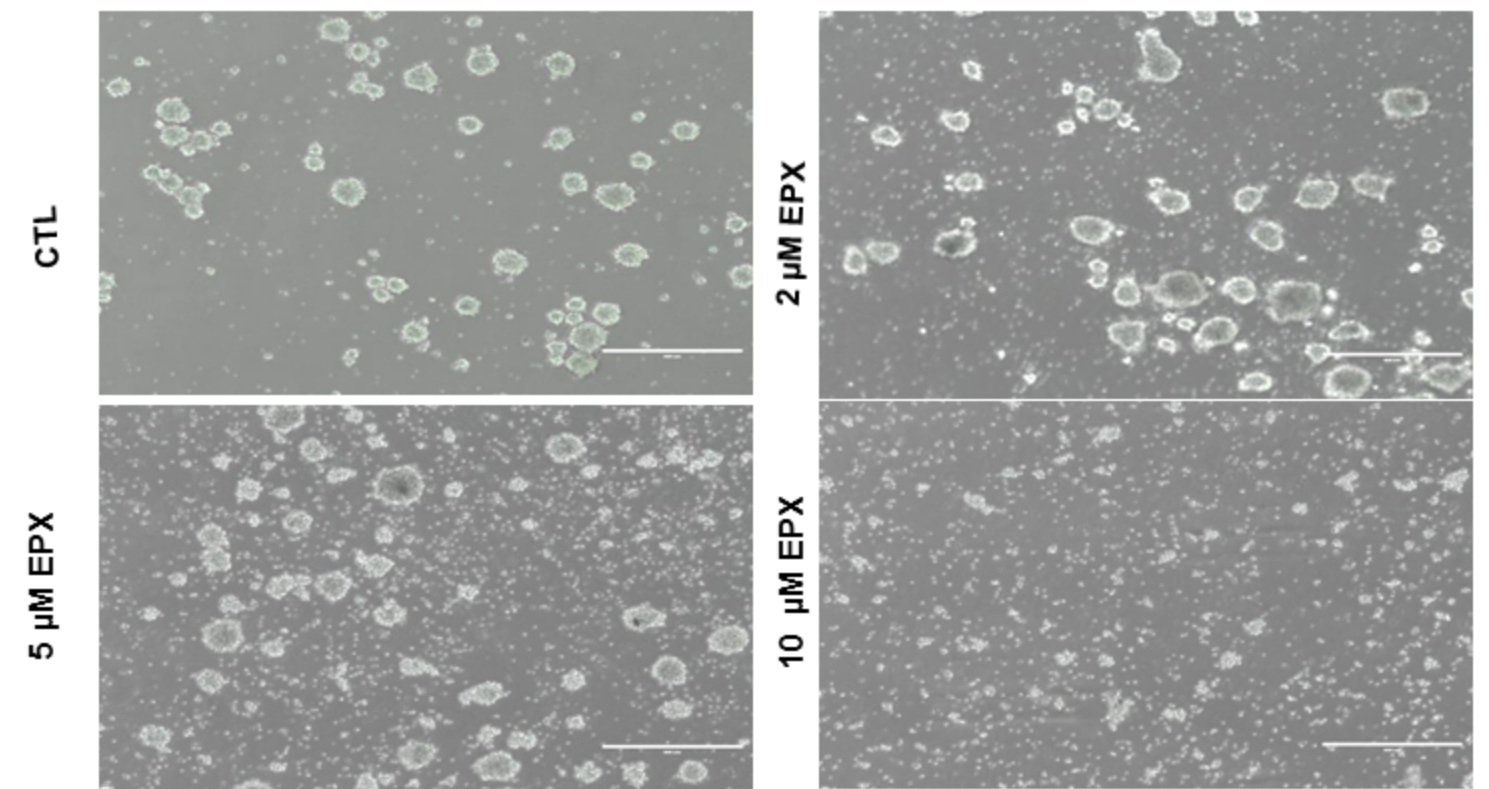
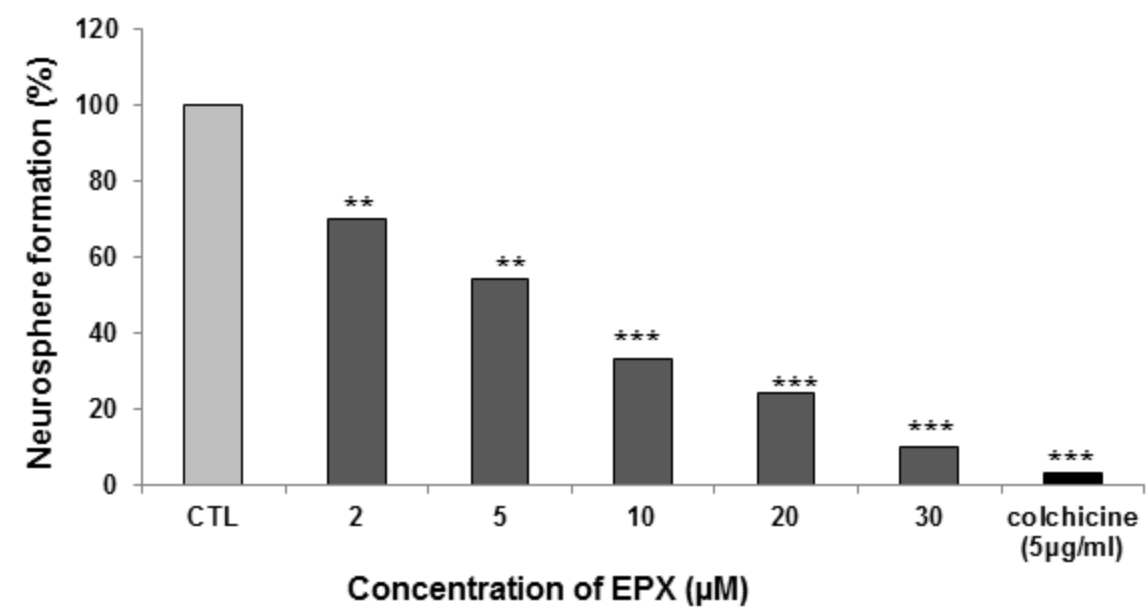
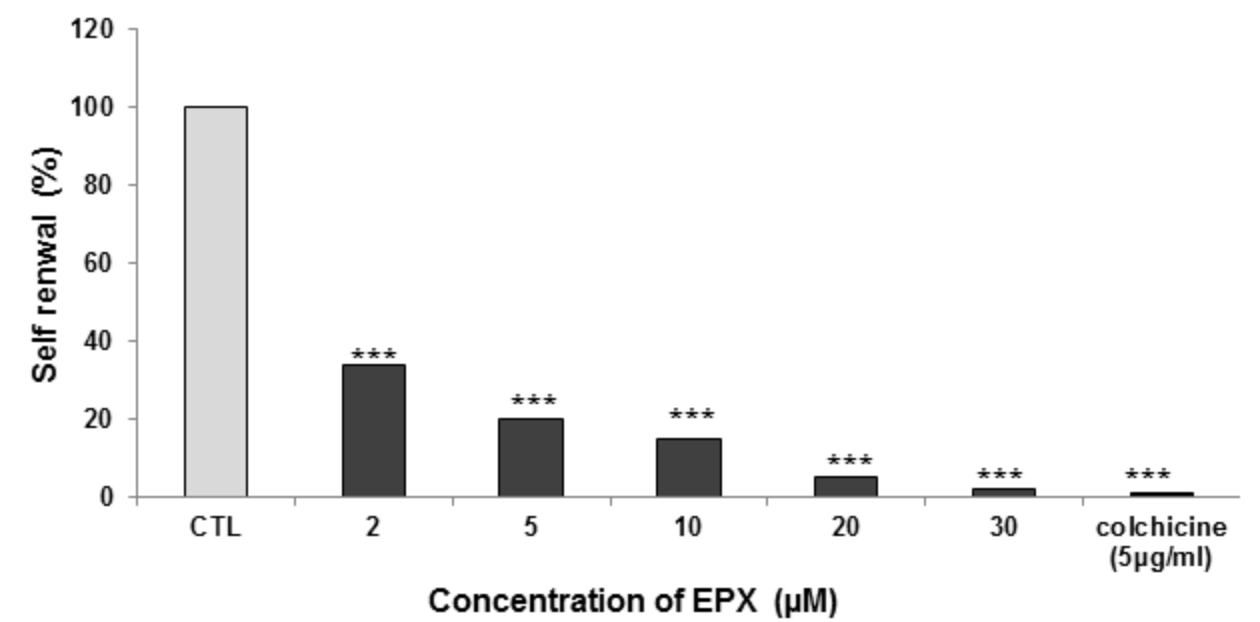
(-) none, (+) mild, (++) moderate, (+++) severe.

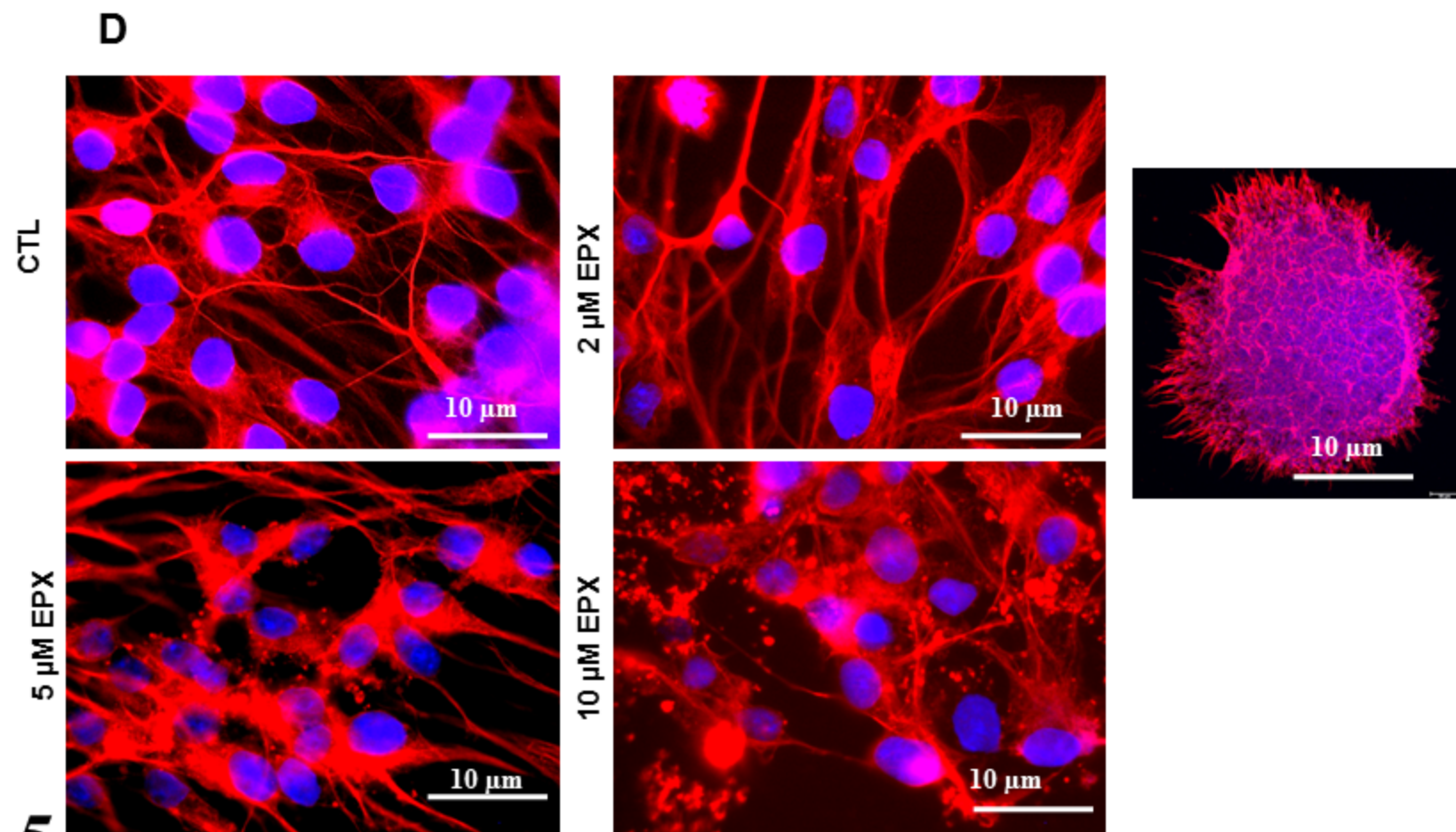
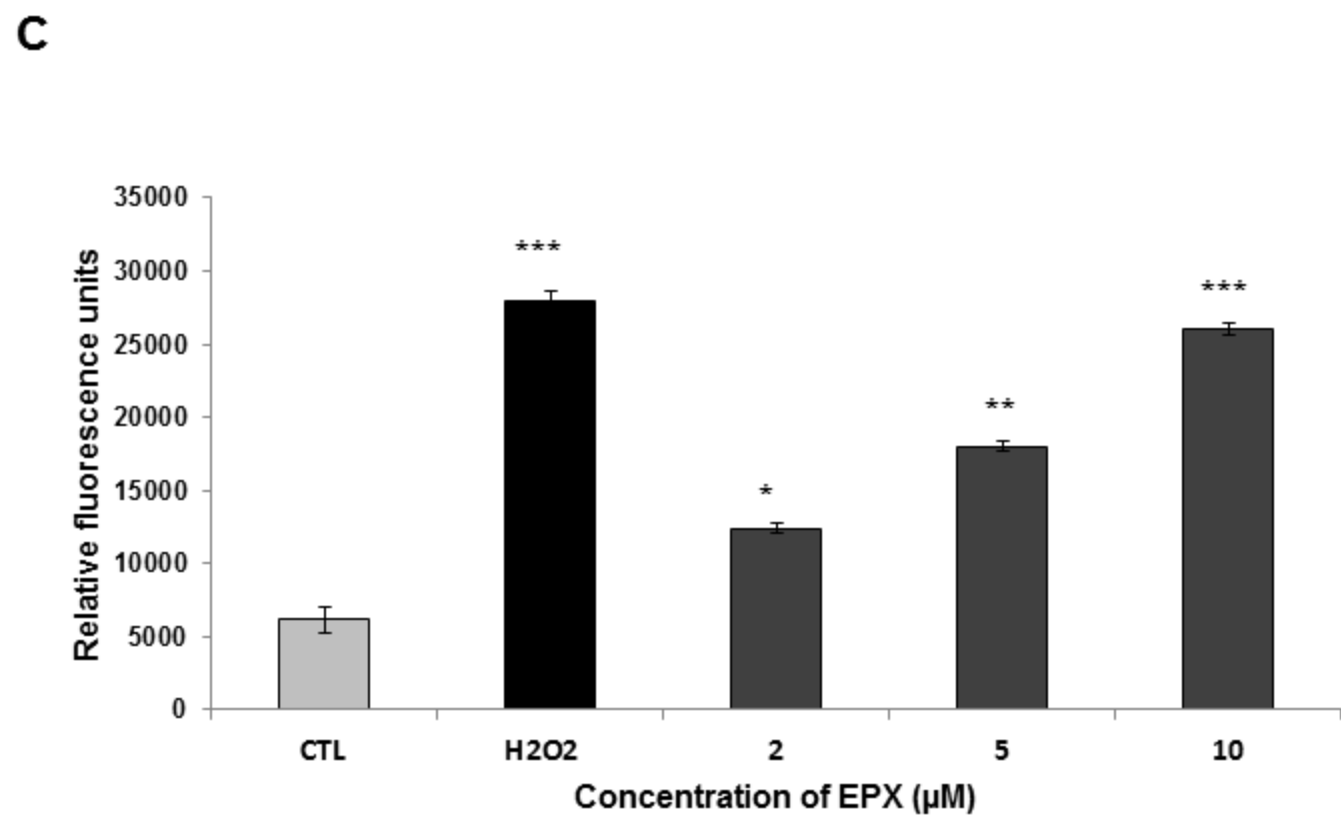
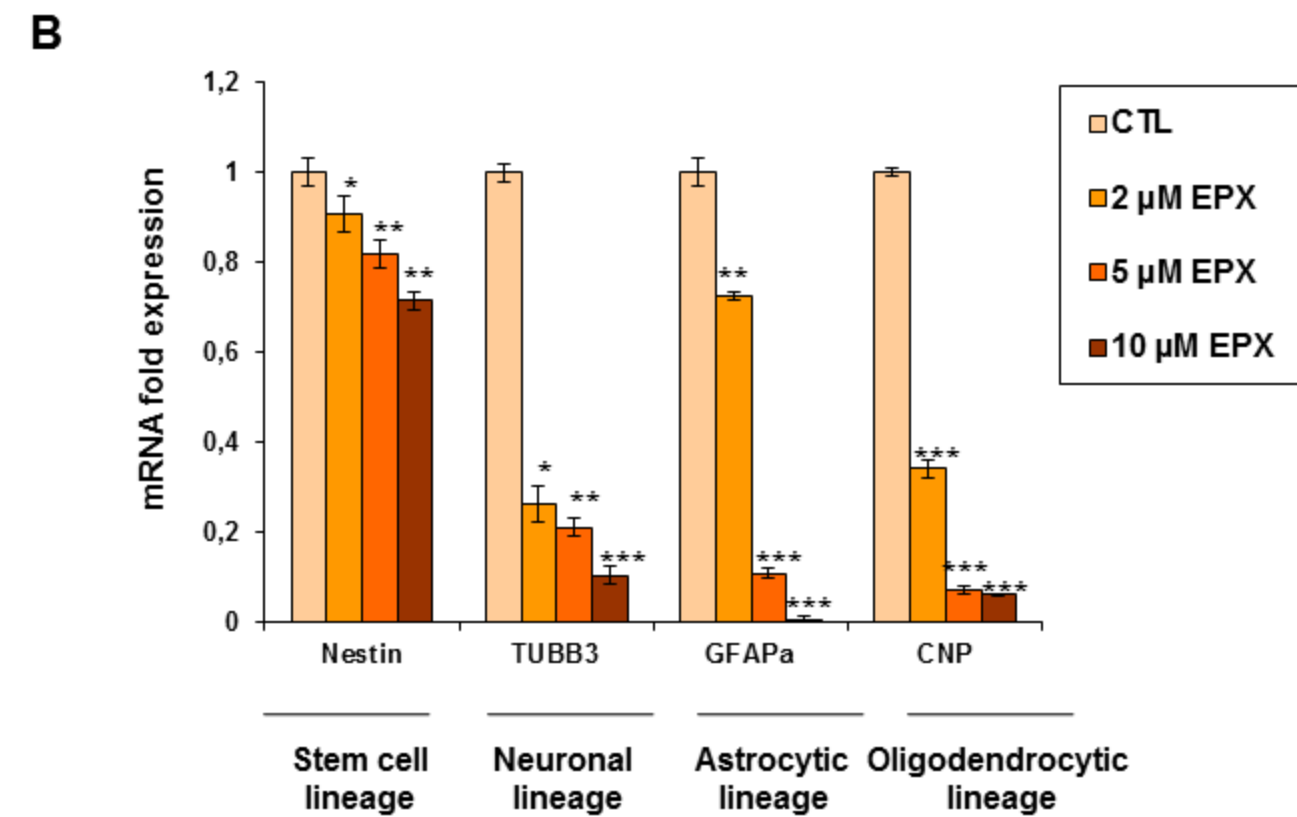
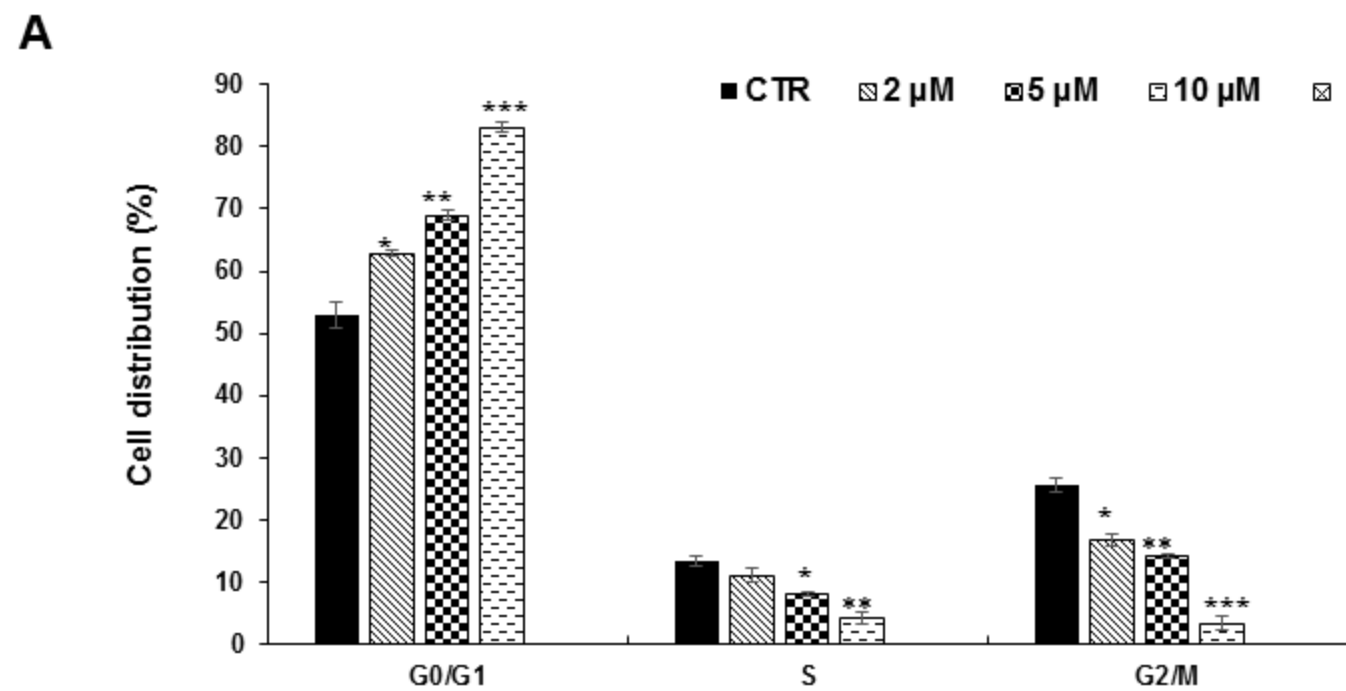


**Fig. 1**

**A****B****C****D****Fig. 2**

**A****B****Fig. 3**

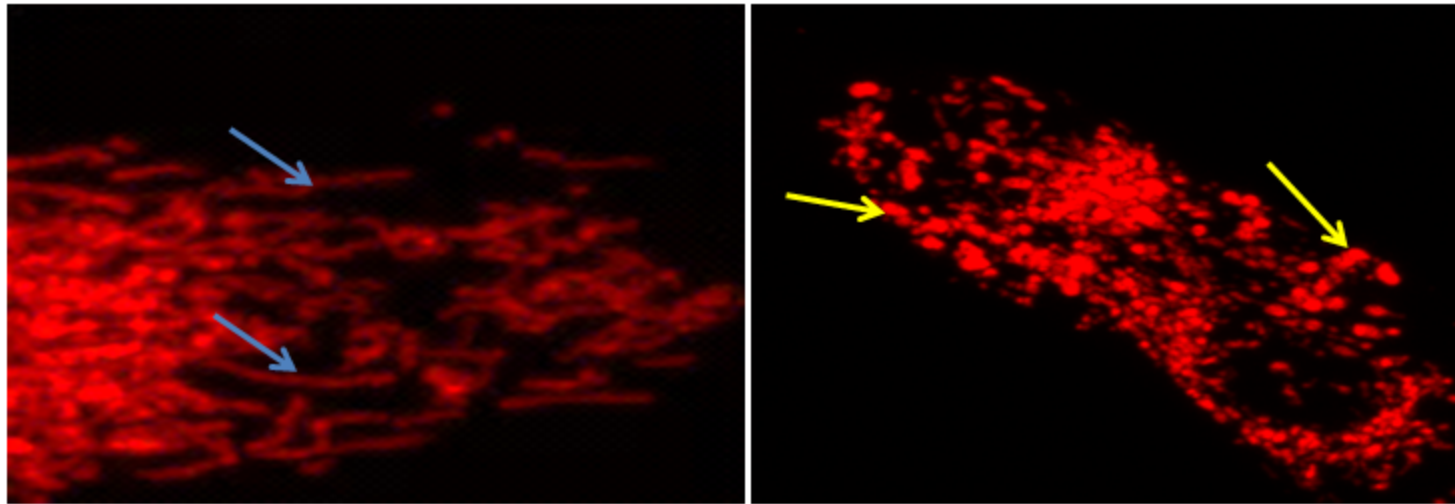
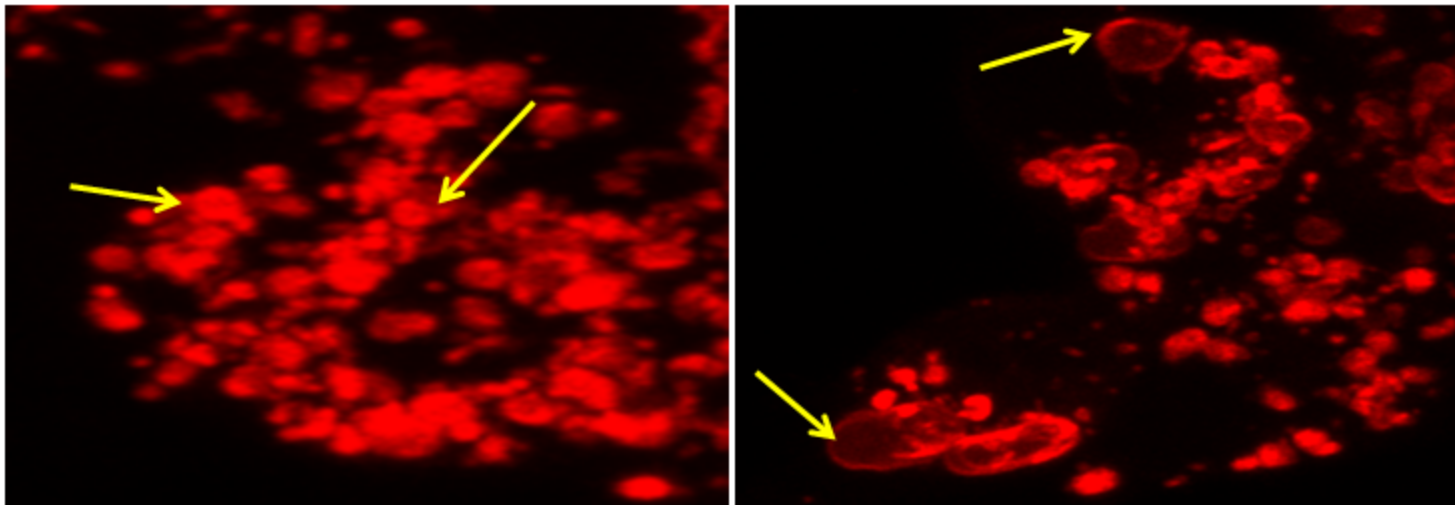
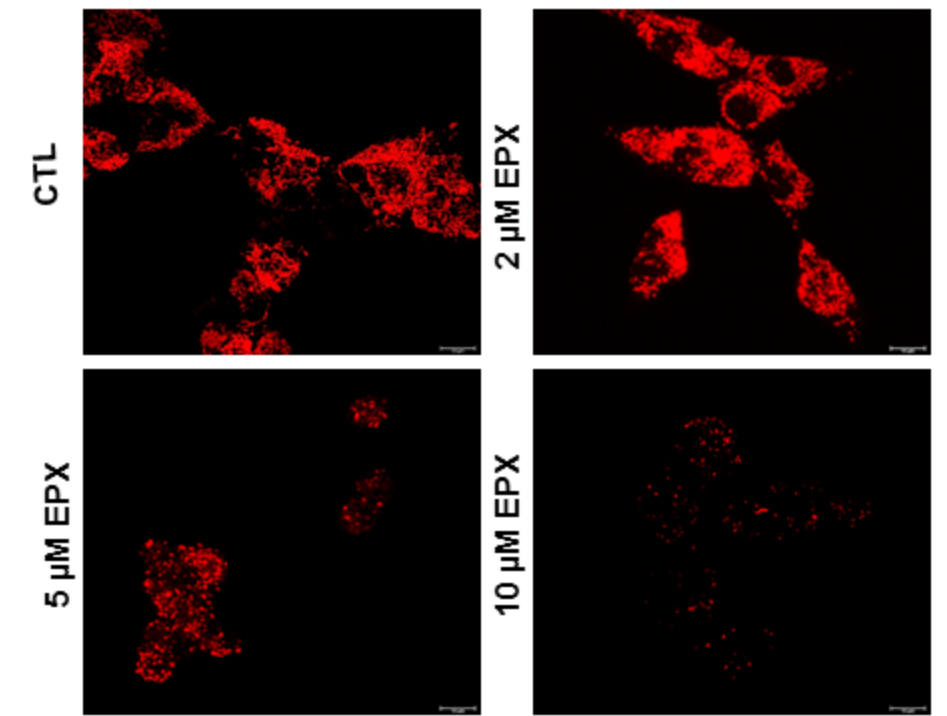
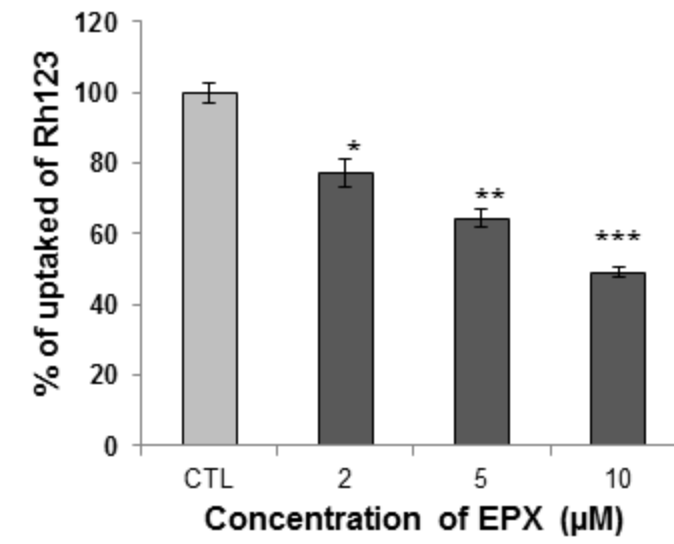
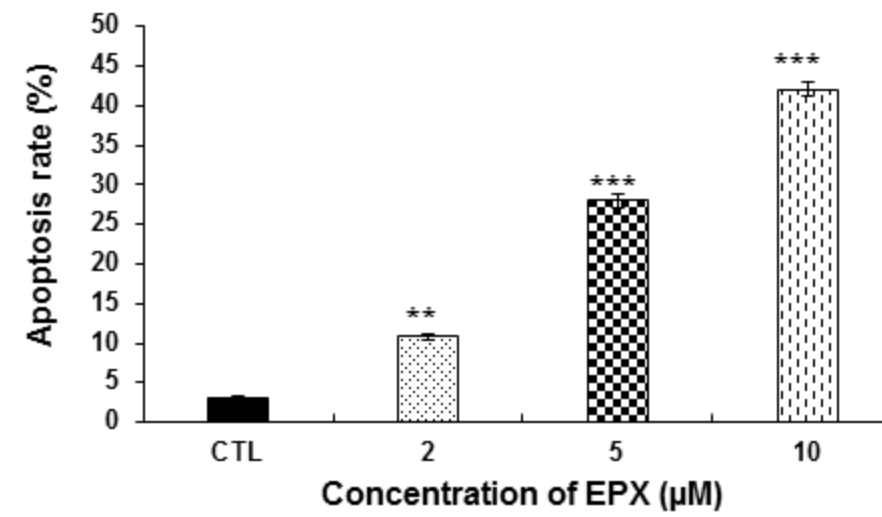
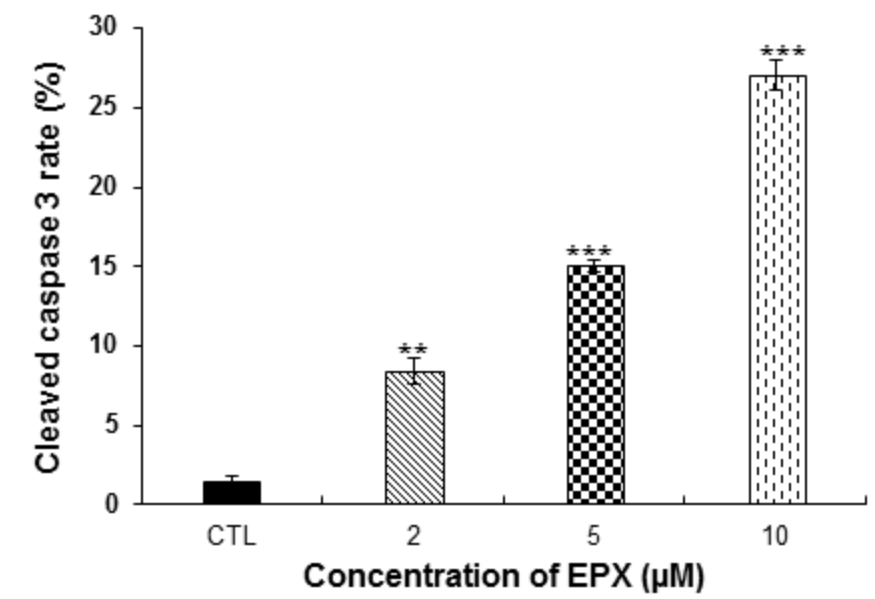
**A****B****C****D****Fig. 4**



**Fig. 5**

**A**

CTL

2  $\mu$ M EPX5  $\mu$ M EPX10  $\mu$ M EPX**B****C****D****Fig. 6**

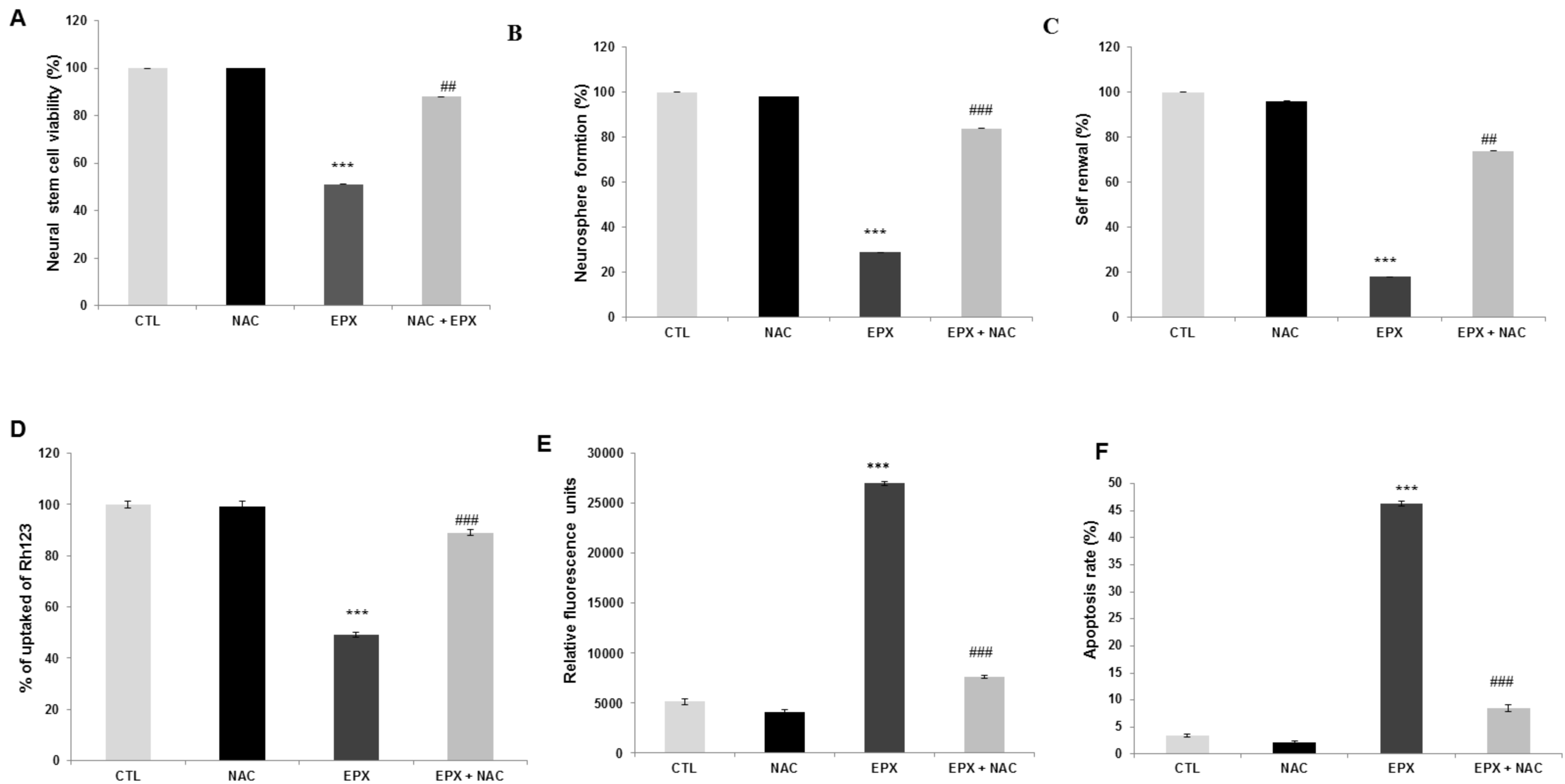


**Fig. 7**